Abstract of the Thesis of

Kevin Grantham for the **Master of Science Degree** in **Physical Science, Physics Emphasis** presented on **July 10, 2006**.

Title: **Approximation of the Magnetic Field of a Circular Loop of Wire**

Abstract approved:

For a current-carrying, circular loop of wire, there is no known method of solving the Biot-Savart law for the exact magnetic field at all points in space. By using a many-sided, regular, polygonal loop to approximate a circular loop, it is possible to solve the Biot-Savart law for the polygon and find an approximate value of the magnetic field for a circular loop. This method is checked for validity against the exact solution for the axial field of a circular loop and two known approximate solutions. The results from the polygonal approximation are found to be within acceptable error limits.

Approximation of the Magnetic Field of a Circular Loop of Wire

----

A Thesis

Presented to

The Departments of Physical Sciences

EMPORIA STATE UNIVERSITY

In Partial Fulfillment

of the Requirement for the Degree

Masters of Science

----

by

Kevin Kale Grantham

July 2006
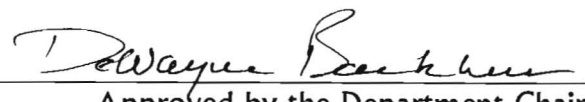
_____
Approved by the Department Chair

_____
Committee Member
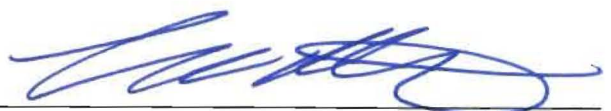
_____
Committee Member

_____
Committee Chair
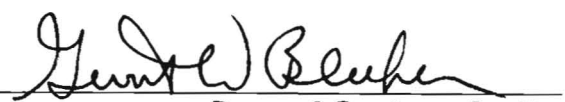
_____
Dean of Graduate Studies

Table of Contents

<u>Chapter</u>

Table of Figures

Chapter 1

Introduction

The belief that there is a relationship between electricity and magnetism may go back as far as Thales (Meyer 46), a Greek philosopher around 600 B.C. It is known that Thales studied electric and magnetic effects. However, it is not known for sure to what extent he studied them since none of his writings have survived (Knierim).

By the late 18th century there was mounting evidence that electricity and magnetism were somehow related. Benjamin Franklin had observed magnetic effects caused by lightning. Pieces of steel were magnetized by lightning and discharges from electrical machines. Boze reported that he had reversed and destroyed the polarity of a magnet through the use of electricity (Meyer 46). Beccaria proposed that the magnetic properties of the Earth were caused by the flow of an "electric fluid" flowing around the Earth (Meyer 46).

In 1819, while performing a demonstration for his students, Hans Oersted, a Danish physicist, noticed that a compass placed near a wire was deflected when he closed the circuit (Weisstein[c]). This discovery is thought to have been an accident, but it probably wasn't for two reasons. First, Oersted studied *Naturphilosophie* under Schelling and believed that all of nature was interconnected. This view could have motivated Oersted to place the compass near the wire to show that the two seemingly different phenomena were more closely related than previously thought (Weisstein[c]). Another reason why Oersted probably did not come upon this discovery by accident was that Romagnosi had discovered the same effect seventeen years earlier. However,

Romagnosi did not pursue this discovery any further and allowed Oersted to take credit

for showing that a current carrying wire creates a magnetic field (Meyer).

After Oersted published his findings in 1820, there was a flood of physicists

researching this newfound relationship (Meyer 48). Most notable of these were the

French physicists Jean Baptiste Biot, Felix Savart and Andre Ampere, and the English

physicist Michael Faraday.

Jean Baptiste Biot, in collaboration with Felix Savart, developed the first

mathematical description of what is now called the magnetic field. However, the modern

field description of electric and magnetic phenomena did not come about until 1845 with

the work of Michael Faraday (Weisstein[b]).

Biot and Savart's initial work was with a long straight wire. They found that, in

modern SI units, the magnitude of the magnetic field follows the equation

$$\left|\vec{B}\right| = \frac{\mu_0 I}{2\pi r} \tag{1-1}$$

where $\left|\vec{B}\right|$ is the magnetic field strength, I is the current, and r is the perpendicular

distance from the wire (Meyer 49). Equation 1-1 is a specific case of the general

equation

$$\vec{B}(r_2) = \frac{\mu_0 I}{4\pi} \oint \frac{d\vec{l} \times (\vec{r}_2 - \vec{r}_1)}{\left|\vec{r}_2 - \vec{r}_1\right|^3} \tag{1-2}$$

where $d\bar{l}$ is a vector length element of the wire, $\bar{r}_1$ is the vector position of $d\bar{l}$, $\bar{r}_2$ is the vector position of the point where the magnetic field is to be calculated, and I is the current through the wire.

Equation 1-2 assumes that the current is along a single line. A more general version of Equation 1-2 is to assume that the current is spread over a volume. In this case, Equation 1-2 needs to be written in terms of a current density $\bar{J}(\bar{r})$:

$$\bar{B}(r_2) = \frac{\mu_0}{4\pi} \oint \frac{\bar{J}(\bar{r}) \times (\bar{r}_2 - \bar{r}_1)}{\left|\bar{r}_2 - \bar{r}_1\right|^3} \, dV \,. \qquad (1\text{-}3)$$

Equation 1-3 is generally called the Biot-Savart law, but it is sometimes called Ampere's law, or in its non-vector form, LaPlace's formula. The name Ampere's law, however, is usually reserved for the following related equation:

$$\bar{\nabla}_2 \times \bar{B}(\bar{r}_2) = \mu_0 \bar{J}. \qquad (1\text{-}4)$$

This is the differential form of Ampere's law. Sometimes it is useful to express Ampere's law in integral form. This can be done by integrating each side of Equation 1-4 over a surface that crosses the path of the current. (This surface is referred to as an Amperian surface.) Then apply Stoke's theorem to get

$$\oint_C \bar{B} \cdot d\bar{l} = \mu_0 \int_S \bar{J} \cdot d\bar{A} \qquad (1\text{-}5)$$

where $d\vec{A}$ is a vector in the direction normal to the surface whose magnitude is a differential area of the Amperian surface, and $d\vec{l}$ is a differential length along the perimeter of the Amperian surface. For a single wire, Equation 1-5 simplifies to

$$\oint_C \vec{B} \cdot d\vec{l} = \mu_0 I .$$
(1-6)

This is the form of Ampere's law that is usually seen in introductory textbooks.

Andre Ampere's work very closely paralleled the work of Biot and Savart. Though Ampere's work was more thorough, he found the same relationship between currents and magnetic induction (Jackson 169). In fact, Ampere's Law can be derived from the Biot-Savart law (Reitz et al 204-205).

The biggest difference between Ampere's work and the work of Biot and Savart is that Biot and Savart dealt with finding the relation between current and $\vec{B}$ directly. Ampere found this relation by studying the forces on adjacent current carrying wires.

Now there is a question of what is the direction of the magnetic field around a current carrying wire. Ampere believed that the magnetic field was radial like the electric field. This idea was later disproved by Michael Faraday who showed that magnetic fields form concentric loops around a current carrying wire (Weisstein[a]).

A drawback of the Biot-Savart law is that, while it is true for all points in space, in practice it can only be applied when there is a symmetry that simplifies the integration. Typical examples include the field of a straight wire and the axial field of a circular loop or solenoid. In cases where there is not sufficient simplifying symmetry to allow the Biot-Savart law to be solved, approximations have to be used.

The scope of this research concentrates on the magnetic field of a circular loop of wire, particularly the off-axis field. There is no analytic solution to the Boit-Savart law for the off axis field. However, an approximate solution can be found by geometrically approximating the circular loop with a many-sided regular polygon. The individual contributions of each side of the polygonal loop can be added to find the approximate field produced by a circular loop (Grivich and Jackson).

Chapter 2

Theory: Approximating the Magnetic Field of a Circular Loop

For a circular loop of wire, the Biot-Savart law can only be solved analytically on the axis. The only region where an analytic solution exists is along the axis of the circular loop. For all other points, a numerical approximation must be found. In this chapter, one method of performing this approximation will be discussed.

One such numerical solution is to approximate the circular loop geometrically. In geometry, one way to define a circle is a regular polygon with an infinite number of sides and whose interior angles are equal to 180 degrees. This definition is not very instructive in visualizing a circle, but in terms of finding a way to geometrically approximate a circle with a regular polygon, this is a good way to view a circle.

Consider the interior angles of a regular polygon. The relationship between the interior angle θ_{int} and the number of sides n in that polygon is as follows:

$$\theta_{int} = 180 - \frac{360}{n}.$$ (2-1)

From this equation it is evident that as the number of sides increases the interior angles start at 60 degrees for an equilateral triangle ($n=3$) and asymptotically approach 180 degrees quickly (Figure 2). The closer the interior angles are to 180 degrees the better the polygon approximates a circle.

This method of approximating the magnetic field of a circular loop has two main strengths. First, a circular loop can be approximated by a polygon with relatively few

sides. Also, the polygonal loop is made up of many straight wire segments which allows for the magnetic field to be calculated at all points in space.

Section 2-1

Calculating the magnetic field of a straight wire segment

What is the magnetic field at some arbitrary point P created by a straight, current carrying wire segment oriented along the x-axis (Figure 3)? The solution can be found on page 866 of Serway's <u>Physics for Scientists and Engineers</u>.

Start with the Biot-Savart law,

$$\bar{B} = \frac{\mu_0 I}{4\pi} \int \frac{d\bar{s} \times \hat{r}}{r^2}. \qquad (2\text{-}2)$$

Because there is cylindrical symmetry, assume that the point of calculation is in the x-y plane. So, the cross product is

$$d\bar{s} \times \hat{r} = \hat{k} \cdot dx \sin\theta. \qquad (2\text{-}3)$$

Substitute this result into Equation 2:

$$\bar{B} = \hat{k} \frac{\mu_0 I}{4\pi} \int \frac{dx \sin\theta}{r^2}. \qquad (2\text{-}4)$$

Since r and θ depend on x, this integral cannot be evaluated unless the integrand is in terms of just one variable. The following relationships will allow Equation 4 to be integrated:

$$r = \frac{a}{\sin \theta} = a \csc \theta \,, \qquad (2\text{-}5)$$

$$x = x_p - \frac{a}{\tan \theta} \qquad (2\text{-}6)$$

where x_p is the x coordinate of the point of calculation (POC). So,

$$dx = a \cdot d\theta \cdot \csc^2 \theta \,. \qquad (2\text{-}7)$$

Substitute Equation 5 and Equation 7 into Equation 4 to get

$$\bar{B} = \hat{k} \frac{\mu_0 I}{4\pi} \int \frac{a \csc^2 \theta \cdot \sin \theta \cdot d\theta}{(a \csc \theta)^2} \,. \qquad (2\text{-}8)$$

This simplifies to

$$\bar{B} = \hat{k} \frac{\mu_0 I}{4\pi a} \int_{\theta_1}^{\theta_2} \sin \theta \cdot d\theta \,. \qquad (2\text{-}9)$$

This integrates to

$$\vec{B} = \hat{k}\,\frac{\mu_0 I}{4\pi\,a}\left(\cos\theta_1 - \cos\theta_2\right) \qquad (2\text{-}10)$$

where the variable a is the perpendicular distance between the wire segment and the POC.

Equation 10 is a compact solution, but what are the cosines? To answer this question, the first thing to do is to define some vectors. Two of these vectors, $\vec{A}_1$ and $\vec{A}_2$, originate at the point of calculation and terminate at the ends of the wire segment. Another vector $\vec{\beta}$ corresponds to the wire segment itself. These three vectors form a triangle. θ_1 is an interior angle of this triangle and the angle between $\vec{A}_1$ and $\vec{\beta}$. So

$$\cos\theta_1 = -\frac{\vec{A}_1 \cdot \vec{\beta}}{\left|\vec{A}_1\right| \cdot \left|\vec{\beta}\right|} \qquad (2\text{-}11)$$

θ_2 is the exterior angle between $\vec{A}_2$ and $\vec{\beta}$.

$$\cos\theta_2 = \frac{\vec{A}_2 \cdot \vec{\beta}}{\left|\vec{A}_2\right| \cdot \left|\vec{\beta}\right|} \qquad (2\text{-}12)$$

It might be easier to describe the angles in terms of coordinates instead of vectors or angles. The wire segment originates at the origin and terminates at $x=l$. The point of calculation is at the point (x, y). Given this configuration, then:

$$\cos\theta_1 = \frac{x}{\left(x^2 + y^2\right)^{1/2}}, \tag{2-13}$$

$$\cos\theta_2 = \frac{(x-l)}{\left[(x-l)^2 + y^2\right]^{1/2}}. \tag{2-14}$$

If Equation 13 and Equation 14 are substituted into Equation 10, and remembering that $y=a$, we get:

$$\vec{B} = \hat{k}\,\frac{\mu_0 I}{4\pi\, y}\left(\frac{x}{\left(x^2 + y^2\right)^{1/2}} - \frac{(x-l)}{\left[(x-l)^2 + y^2\right]^{1/2}}\right). \tag{2-15}$$

Now we have an equation for the magnetic field of a straight wire segment that is put in terms of the coordinates of the POC.

It would be interesting to look at a couple of graphs of this equation. The first graph is B vs. x with constant y (Figures 4 and 5). Then there are a couple of graphs of B vs. y with constant x that are of interest. One is with x such that the graph crosses the wire segment (Figure 6). The other graph is such that the x is outside the wire segment (Figure 7). Since we are only interested in the behavior of the magnetic field as the coordinate changes, in the graphs all the constants in Equation 15 are set to 1. These graphs show how the magnetic field around a wire segment behaves.

In order to compute the magnetic field for a current carrying polygon, it is important to know how to relate the coordinate systems to each other. The next section

will discuss how to relate a coordinate system defined by a side of a polygonal loop to the coordinate system defined by the center of the loop.

Section 2-2

Translating and rotating coordinate systems

In the last chapter, an equation to calculate the magnetic field of a straight current carrying wire placed along the x-axis from $x = 0$ to $x = l$ was derived. This equation is in terms of the coordinates of the POC (point of calculation). If the current-carrying wire is not oriented along the x-axis (e.g., the sides of a current-carrying regular polygon centered at the origin), it is possible through translations and rotations to create a coordinate system to match the conditions assumed in Chapter 2. This section steps through finding that coordinate system.

Take a straight wire segment placed randomly in the x-y plane. The current in the wire originates at (x_1, y_1) and terminates at (x_2, y_2). Define the angle θ to be the angle between the wire segment and the positive x-axis.

The conditions assumed in Chapter 2 are that the origin is the point of origin of the current in the wire segment, and the x-axis is parallel to the wire segment. This defines the coordinate system that is translated and rotated from the original coordinate system in which the magnetic field is easily calculated. However, the end points of the wire segment and the POC are defined in the original coordinate system. So what are the coordinates of the end points and the POC in this new coordinate system (Figure 8)?

For initial simplicity, assume that the POC is in the x-y plane. With this condition the magnitude of the magnetic field can be found with only one translation and one

rotation. The direction of the magnetic field is also defined by this condition to be in the $\pm z$ direction. The positions of the end points of the wire segment in the new coordinate system can be found by examination of the conditions for calculation. The point (x_1, y_1) becomes the origin in the new coordinate system. The point (x_2, y_2) becomes the point $(l, 0)$ in the new coordinate system.

The coordinates of the POC in the new coordinate system are not as easily found as the coordinates of the endpoints. The translation and rotation have to be applied to the POC. In the original coordinate system, the position of the POC will be labeled (x_0, y_0).

First translate the original coordinate system to create a primed coordinate system in which the origin has been moved to (x_1, y_1). In this coordinate system the x-component of the POC position will become

$$x' = x_1 - x_0 . \tag{2-16}$$

The y component of position becomes

$$y' = y_1 - y_0 . \tag{2-17}$$

Since the translation is only in the x-y plane, it doesn't affect the z-component of the POC:

$$z' = z . \tag{2-18}$$

Now the primed coordinate system has to be rotated by an angle of θ to align the wire segment along the positive x-axis. The coordinate system is being rotated about the z-axis so the z-component is unchanged. To find the x- and y-components in this double-primed coordinate system we have to apply a rotation matrix to the primed position vector of the POC:

$$\begin{pmatrix} x'' \\ y'' \end{pmatrix} = \begin{pmatrix} x' \\ y' \end{pmatrix} \begin{pmatrix} \cos\theta & \sin\theta \\ -\sin\theta & \cos\theta \end{pmatrix}. \tag{2-19}$$

So,

$$x'' = x'\cos\theta + y'\sin\theta, \tag{2-20}$$

$$y'' = -x'\sin\theta + y'\cos\theta, \tag{2-21}$$

$$z'' = z \tag{2-22}$$

Or in terms of the original coordinate system

$$x'' = (x_1 - x_0)\cos\theta + (y_1 - y_0)\sin\theta, \tag{2-23}$$

$$y'' = -(x_1 - x_0)\sin\theta + (y_1 - y_0)\cos\theta, \tag{2-24}$$

$$z'' = z. \tag{2-25}$$

θ can be put in terms of the coordinates. This gives

$$x'' = \frac{(x_1 - x_0)(x_2 - x_1)}{\left((x_2 - x_1)^2 + (y_2 - y_1)^2\right)^{1/2}} + \frac{(y_1 - y_0)(y_2 - y_1)}{\left((x_2 - x_1)^2 + (y_2 - y_1)^2\right)^{1/2}}, \qquad (2\text{-}26)$$

$$y'' = -\frac{(x_1 - x_0)(y_2 - y_1)}{\left((x_2 - x_1)^2 + (y_2 - y_1)^2\right)^{1/2}} + \frac{(x_2 - x_1)(y_1 - y_0)}{\left((x_2 - x_1)^2 + (y_2 - y_1)^2\right)^{1/2}}, \qquad (2\text{-}27)$$

$$z'' = z. \qquad (2\text{-}28)$$

This result assumes that the POC and the wire segment are in a plane that is parallel to the x-y plane. If the POC has a z-coordinate that is different than the z-coordinate of the wire segment, another rotation is needed. This time the rotation is around the $x'' - $ axis.

This rotation can be done using a rotation matrix similar to that in Equation 4, but there is a much simpler way. Since the rotation is around the $x'' - $ axis, the $x'' - $ coordinate does not change. From the conditions for calculation we know that $z''' = 0$. The $y''' - $ coordinate is simply the perpendicular distance between the POC and the wire segment.

So,

$$x''' = \frac{(x_1 - x_0)(x_2 - x_1)}{\left((x_2 - x_1)^2 + (y_2 - y_1)^2\right)^{1/2}} + \frac{(y_1 - y_0)(y_2 - y_1)}{\left((x_2 - x_1)^2 + (y_2 - y_1)^2\right)^{1/2}}, \qquad (2\text{-}29)$$

$$y''' = \left\{ \left[-\frac{(x_1 - x_0)(y_2 - y_1)}{\left((x_2 - x_1)^2 + (y_2 - y_1)^2\right)^{1/2}} + \frac{(x_2 - x_1)(y_1 - y_0)}{\left((x_2 - x_1)^2 + (y_2 - y_1)^2\right)^{1/2}} \right]^2 + [z_1 - z_0]^2 \right\}^{1/2} , \quad (2\text{-}30)$$

$$z''' = 0 . \qquad (2\text{-}31)$$

This can now be substituted into Equation 2-15 for the magnetic field of a straight wire segment:

$$B = \frac{\mu_0 I}{4\pi y'''} \left(\frac{x'''}{\left(x'''^2 + y'''^2\right)^{1/2}} - \frac{(x''' - l)}{\left[(x''' - l)^2 + y'''^2\right]^{1/2}} \right). \qquad (2\text{-}32)$$

This gives the magnitude of the magnetic field at any position relative to a straight wire segment provided the wire segment is parallel to the x-y plane.

The direction of the magnetic field is in the z''' direction, but what is the direction in the unprimed coordinate system? This can be found using a cross product. The first vector of the cross product is the vector that connects the POC to the point of origin of the wire segment. This vector will be referred to as $\vec{P}$:

$$\vec{P} = (x_0 - x_1)\hat{i} + (y_0 - y_1)\hat{j} + (z_0 - z_1)\hat{k} . \qquad (2\text{-}33)$$

The second vector in the cross product is a vector that corresponds to the wire segment labeled $\vec{S}$:

$$\vec{S} = \left(x_2 - x_1\right)\hat{i} + \left(y_2 - y_1\right)\hat{j} + \left(z_2 - z_1\right)\hat{k}. \tag{2-34}$$

A unit vector in the same direction as this cross product gives the direction of the magnetic field at the POC. So the transformation of $\hat{z}'''$ into the unprimed coordinate system is

$$\hat{z}''' = \frac{\vec{P} \times \vec{S}}{\left\|\vec{P} \times \vec{S}\right\|}. \tag{2-35}$$

So the magnetic field at POC is

$$\vec{B} = \frac{\mu_0 I}{4\pi y'''}\left(\frac{x'''}{\left(x'''^2 + y'''^2\right)^{1/2}} - \frac{\left(x''' - l\right)}{\left[\left(x''' - l\right)^2 + y'''^2\right]^{1/2}}\right) \cdot \frac{\vec{P} \times \vec{S}}{\left\|\vec{P} \times \vec{S}\right\|}. \tag{2-36}$$

By making the necessary substitutions to put $x''', y''', \vec{P}$ and $\vec{S}$ in terms of the unprimed coordinate system, it is obvious that this is a tedious calculation. If there is only one wire segment, this idea of using rotations and translation does not make a lot of sense because the coordinate system can be chosen to simplify the magnetic field calculation. When there is more than one wire segment (i.e., a regular polygon), this technique is necessary in order to find the position of the POC relative to each wire segment.

Section 2-3

A program in MATLAB to calculate the magnetic field

For a regular polygon the calculation of the magnetic field is tedious due to the calculation having to be performed several times (once for each side of the polygon). For a polygonal loop that is used to approximate a circular loop, the tedium increases with the addition of each side. More sides added to the polygon results in a better approximation to a circle, but it also results in a significant number of manual calculations. One way to alleviate the tedium involved in performing these calculations manually is to write a computer algorithm to perform them. This allows for the magnetic field to be calculated in a fraction of the time it would take to do it manually.

The following is a listing of MATLAB code that performs the required calculations to approximate the magnetic field of any regular polygon, centered about the z-axis. The comments in the code (shown in green and proceeded by a percent sign) explain the function of each section of the program.

```
% singlecalc1 - A program that calculates the magnetic field of a
regular polygonal loop centered about the z-axis
clear;  help singlecalc1;
%The first couple of lines initialize the program.


%This section defines mu and asks for user-defined conditions for the
calculation.
mu = 4*pi*10^(-7)
n = input('Enter number of sides   ')
r = input('Enter the radius in meters ')
N = input('enter the number of turns  ')
I = input('enter the current in Amperes  ')
xcord = input('enter the x coordinate   ')
ycord = input('enter the y coordinate   ')
z = input('enter the z coordinate   ')


i=0;
j=1;
```

```
1   %This loop produces an nx3 matrix.  Each row of this matrix
    corresponds to the coordinates of each vertex of the polygon.
2   %This loop also initializes the matrix tic that will later be a
    list of direction vectors.
3   while i<n
4   A(i+1,:)= [r*cos(2*i*pi/n), r*sin(2*i*pi/n), 0];
5   tic(i+1,:)= [i i i];
6   i=i+1;
7   end
8   i=0;

9   %This section returns an nx3 matrix.  Each row each row
    corresponds to a vector that represents each side of the polygon
10  %The direction of these vectors indicate the direction of the
    current.
11  while i<n-1
12  side(i+1,:)=A(i+2,:)-A(i+1,:);
13  i=i+1;
14  end
15  side(n,:)=A(1,:)-A(n,:);
16  i=0;

17  %This loop calculates the length of each side and returns an nx1
    matrix listing the length of each side.
18  %Since the loop is a regular polygon, each row of this matrix is
    the same.
19  while i<n
20  L(i+1,:)=sqrt(sum(side(i+1,:).^2));
21  i=i+1;
22  end
23  i=0;

24  %The nx1 matrix theta is a list of the angles of each side of the
    polygon relative to the positive x-axis.
25  %Note that when i=0, the angle calculated does not correspond to
    the first side of the polygon.
26  %The way this issue was resolved is subtle and will be pointed
    out.
27  while i<n
28  theta(i+1,:)=pi/2-pi/n+i*2*pi/n;
29  i=i+1;
30  end
31  i=0;

32  %Now the translation, rotation, and calculation of the magnetic
    field can be performed.
33  while i<n
34  k=0;

35  %This loop translates and rotates coordinate system to find the
    location of the POC relative to each side of the polygon.
36  %The angle matrix theta starts on the nth side. The first
    translation assumes that theta start at the first side.
37  %This discrepancy is partially resolved by rotating the
    coordinate systems an additional 180 degrees.
38  %The problem is only partially resolved because now there is a
    sign problem.
```

```
39 while k<n
40 xcord_1(k+1,:)= A(k+1,1)-xcord;
41 ycord_1(k+1,:)= A(k+1,2)-ycord;
42 xcord_2(k+1,:)=xcord_1(k+1,:)*cos(theta(k+1,:))+ycord_1(k+1,:)*si
   n(theta(k+1,:));
43 ycord_2(k+1,:)=-
   xcord_1(k+1,:)*sin(theta(k+1,:))+ycord_1(k+1,:)*cos(theta(k+1,:))
   ;
44 k=k+1;
45 end
46 k=0;

47 %In this section, a couple of things are calculates. First is an
   nx3 matrix representing the position vectors of the POC in the
   third primed coordinate system for each side.
48 %Second an nx1 matrix of the magnitudes of the previously
   mentioned position vectors
49 %Lastly is an nx3 matrix listing of unit vectors that with a
   little reordering give the direction of each sides contribution
   to the magnetic field.
50 while k<n
51 zcord(k+1,:)=z;
52 cord(k+1,:)=[xcord, ycord, z];
53 magcord(k+1,:)=sqrt(sum(cord(k+1,:).^2));
54 P(k+1,:)=A(k+1,:)-cord(k+1,:);
55 magP(k+1,:)=sqrt(sum(P(k+1,:).^2));
56 perp(k+1,:)=sqrt(ycord_2(k+1,:).^2+zcord(k+1,:).^2);
57 if ycord_2(k+1,:)<0
58 perp(k+1,:)=-1*perp(k+1,:);
59 end
60 kevin(k+1,:)=cross(P(k+1,:),side(k+1,:));
61 direction(k+1,:)=(kevin(k+1,:)./(sqrt(sum(kevin(k+1,:).^2))));
62 k=k+1;
63 end

64 %This is the actual calculation of the magnitude of the magnetic
   field.  The aforementioned sign problem is resolved by switching
   the order of the angles in this calculation.
65 B(i+1,:)=abs(mu*I*N/(4*pi*(perp(i+1,:)))*((xcord_2(i+1,:)-
   L(i+1,:))./sqrt(perp(i+1,:).^2+(xcord_2(i+1,:)-L(i+1,:)).^2) -
   (xcord_2(i+1,:))/sqrt(perp(i+1,:).^2+(xcord_2(i+1,:)).^2)));

66 %This reorders the direction vectors so that direction matches
   the magnetic field calculation
67 if i>0
68 tic(i+1,:)=direction(i,:);
69 else
70 tic(1,:)=direction(n,:);
71 end

72 %The variable b is an nx3 matrix in which each row is the vector
   contribution to the magnetic field for each side.
73 b(i+1,1)=B(i+1,:).*tic(i+1,1);
74 b(i+1,2)=B(i+1,:).*tic(i+1,2);
75 b(i+1,3)=B(i+1,:).*tic(i+1,3);
76 i=i+1;
77 end
```

```
78 %Btot is the total magnetic field of a current carrying polygon
   in Cartesian coordinates
79 Btot(j,1)=sum(b(:,1));
80 Btot(j,2)=sum(b(:,2));
81 Btot(j,3)=sum(b(:,3));

82 %Cartesian coordinates are not very conducive to visualizing the
   magnetic field.
83 %The symmetry of the polygon makes it reasonable to convert into
   cylindrical coordinates.
84 B_R(j,1)=Btot(j,1)*xcord/(sqrt(xcord^2+ycord^2))+Btot(j,2)*ycord/
   (sqrt(xcord^2+ycord^2))
85 B_Theta(j,1)=-
   Btot(j,2)*xcord/(sqrt(xcord^2+ycord^2))+Btot(j,1)*ycord/(sqrt(xco
   rd^2+ycord^2))
86 B_Z(j,1)=Btot(j,3)
```

Section 2-4

Calculations to be used for quantitatively testing the MATLAB code

There are three calculations that can be used to test how well the code from

Section 2-3 approximates the magnetic field of a circular loop. First is the calculation of

the on-axis magnetic field. This is the only region where the magnetic field is known

exactly. The magnetic field can also be approximated at points "far" from the loop. The

last area the MATLAB code can be tested only applies to the radial component of the

magnetic field near the axis of the loop.

Even though the last two regions that will be used to test the code are only

approximations, they are still useful in deciding how well the polygonal approximation

works. The basis for this is that these approximations give results that are close to the

actual value of the magnetic field within the regions where they were meant to be used.

If the polygonal approximation gives acceptable results compared to these

approximations, then there is good reason to believe that the polygonal approximation

also gives acceptable results to the unknown true value in those regions as well.

Section2-4.1

To calculate the on-axis magnetic field of a circular loop start with the Biot-Savart law (Figure 8-5 Reitz, et. al.):

$$\bar{B}(r_2) = \frac{\mu_0}{4\pi} I \oint_1 \frac{dl \times (\bar{r}_2 - \bar{r}_1)}{|\bar{r}_2 - \bar{r}_1|^3}.$$

(2-37)

Make the following substitutions:

$$dl = a(-\hat{i} \sin \theta + \hat{j} \cos \theta) d\theta,$$

$$\bar{r}_2 - \bar{r}_1 = -\hat{i} a \cos \theta - \hat{j} a \sin \theta + \hat{k} z,$$

(2-38)

$$|r_2 - r_1| = (a^2 + z^2)^{1/2}$$

to get

$$\bar{B}(r_2) = \frac{\mu_0}{4\pi} I \int_0^{2\pi} \frac{a(-\hat{i} \sin \theta + \hat{j} \cos \theta) \times (-\hat{i} a \cos \theta - \hat{j} a \sin \theta + \hat{k} z)}{(a^2 + z^2)^{3/2}} d\theta.$$

(2-39)

Performing the cross product in the numerator gives

$$\bar{B}(r_2) = \frac{\mu_0}{4\pi} I \int_0^{2\pi} \frac{(\hat{i} z a \cos \theta + \hat{j} z a \sin \theta + \hat{k} a^2)}{(a^2 + z^2)^{3/2}} d\theta.$$

(2-40)

The $\hat{i}$ and $\hat{j}$ terms of this equation integrate to 0 leaving

$$\bar{B}(r_2) = \hat{k}\frac{\mu_0}{4\pi}I\frac{(a^2)}{(a^2+z^2)^{3/2}}\int_0^{2\pi}d\theta \qquad (2\text{-}41)$$

or

$$\bar{B}(r_2) = \frac{\mu_0 I}{2}\frac{(a^2)}{(a^2+z^2)^{3/2}}\hat{k}. \qquad (2\text{-}42)$$

Equation 2-42 shows the on axis magnetic field of a circular current carrying loop of wire

(Reitz, et. al. 200).

Section 2-4.2

The second calculation that can be used to test the MATLAB code is the

approximation for the radial component near the axis of the current carrying circular loop

(problem 8-12, page 215 in Reitz, et. al.). This is achieved by analyzing the divergence

of the magnetic field. In cylindrical coordinates the divergence of $\bar{B}$ is

$$\nabla\cdot\bar{B} = 0 = \frac{1}{r}\frac{\partial}{\partial r}(rB_r) + \frac{1}{r}\frac{\partial B_\theta}{\partial \theta} + \frac{\partial B_z}{\partial z}. \qquad (2\text{-}43)$$

Due to symmetry

$$\frac{1}{r}\frac{\partial B_\theta}{\partial \theta} = 0. \qquad (2\text{-}44)$$

Therefore,

$$\nabla \cdot \bar{B} = \frac{1}{r}\frac{\partial}{\partial r}(rB_r) + \frac{\partial B_z}{\partial z}. \qquad (2\text{-}45)$$

Now, apply the product rule to the radial component to separate it into two derivatives:

$$\nabla \cdot \bar{B} = \frac{1}{r}B_r + \frac{\partial B_r}{\partial r} + \frac{\partial B_z}{\partial z}. \qquad (2\text{-}46)$$

By Gauss's law, equation 2-46 is equal to zero, so

$$0 = \frac{1}{r}B_r + \frac{\partial B_r}{\partial r} + \frac{\partial B_z}{\partial z}. \qquad (2\text{-}47)$$

Try as a solution to Equation 2-47

$$B_r = c_0 + c_1 r + c_2 r^2 + c_3 r^3 + \dots \qquad (2\text{-}48)$$

where $c_0, c_1, c_2, c_3 \dots$ are functions of z.

As $r \to 0$, the terms higher than the linear term can be neglected. Also, as r goes to zero, B_r must also go to zero. This means that $c_0 = 0$, leaving

$$B_r \approx c_1 r. \qquad (2\text{-}49)$$

Substitute Equation 2-49 and its derivative into Equation 2-47 to find:

$$c_1 = \frac{1}{2} \frac{\partial B_z}{\partial z}.$$

Since r is small, the z-component of the magnetic field is approximately equal to the on-axis field:

$$\bar{B}(r_2) \approx \frac{\mu_0 I}{2} \frac{(a^2)}{(a^2 + z^2)^{3/2}} \hat{k},$$

so

$$\frac{\partial B_z}{\partial z} = \frac{3\mu_0 I}{2} \frac{a^2 z}{(z^2 + a^2)^{5/2}}.$$

Therefore,

$$c_1 = \frac{3\mu_0 I}{4} \frac{a^2 z}{(z^2 + a^2)^{5/2}}, \tag{2-50}$$

so,

$$B_r \approx \frac{3\mu_0 I}{4} \frac{a^2 z r}{(z^2 + a^2)^{5/2}}. \tag{2-51}$$

Equation 2-51 gives an approximate value for the radial component of the magnetic field. The limitation to this approximation is that it only works for $r \ll a$, and there are no available analytical tests to show its accuracy.

Section 2-4.3

The next area in which the MATLAB code can be tested is the magnetic field far from the current carrying loop (Reitz, et. al. 210). Rather than using the Biot-Savart law to approximate the magnetic field, it is easier to start with the vector potential:

$$\bar{A}(\bar{r}_2) = \frac{\mu_0 I}{4\pi} \oint \frac{d\bar{r}_1}{|\bar{r}_2 - \bar{r}_1|}. \tag{2-52}$$

For $r_2 \gg r_1$, the denominator of Equation 2-52 can be approximated by rewriting it as in Equation 2-53 and expanding in powers of r_1/r_2 :

$$\left| \vec{r}_2 - \vec{r}_1 \right|^{-1} = \left(r_2^2 + r_1^2 - 2\vec{r}_1 \cdot \vec{r}_2 \right)^{-1/2} , \tag{2-53}$$

$$\left| \vec{r}_2 - \vec{r}_1 \right|^{-1} = \frac{1}{r_2} \left[1 + \frac{\vec{r}_1 \cdot \vec{r}_2}{r_2^2} + ... \right]. \tag{2-54}$$

Equation 2-54 is the expansion to first order in r_1/r_2 . Substitute this result (2-54) into Equation 2-52 to get

$$\vec{A}(\vec{r}_2) = \frac{\mu_0 I}{4\pi} \left\{ \frac{1}{r_2} \oint d\vec{r}_1 + \frac{1}{r_2^3} \oint d\vec{r}_1 \left(\vec{r}_1 \cdot \vec{r}_2 \right) + ... \right\}. \tag{2-55}$$

The first integral goes to zero and the second integral is one term of

$$\left(\vec{r}_1 \times d\vec{r}_1 \right) \times \vec{r}_2 = -\vec{r}_1 \left(\vec{r}_2 \cdot d\vec{r}_1 \right) + d\vec{r}_1 \left(\vec{r}_1 \cdot \vec{r}_2 \right). \tag{2-56}$$

Consider the differential of $\vec{r}_1 \left(\vec{r}_1 \cdot \vec{r}_2 \right)$ for a small change in $\vec{r}_1$. This is

$$d\left[r_1 \left(\vec{r}_2 \cdot \vec{r}_1 \right) \right] = \vec{r}_1 \left(\vec{r}_2 \cdot d\vec{r}_1 \right) + d\vec{r}_1 \left(\vec{r}_2 \cdot \vec{r}_1 \right). \tag{2-57}$$

Equation 2-57 is an exact differential. If we add Equation 2-56 and equation 2-57

together we can solve for $d\bar{r}_1(\bar{r}_2 \cdot \bar{r}_1)$ to get

$$d\bar{r}_1(\bar{r}_2 \cdot \bar{r}_1) = \frac{1}{2}(\bar{r}_1 \times d\bar{r}_1) \times \bar{r}_2 + \frac{1}{2}d[r_1(\bar{r}_2 \cdot \bar{r}_1)].$$

(2-58)

Substitute Equation 2-58 back into equation 2-55 to get

$$\bar{A}(\bar{r}_2) = \frac{\mu_0 I}{4\pi}\left\{\frac{1}{r_2{}^3}\oint\left[\frac{1}{2}(\bar{r}_1 \times d\bar{r}_1) \times \bar{r}_2 + \frac{1}{2}d[r_1(\bar{r}_2 \cdot \bar{r}_1)]\right]\right\}.$$

(2-59)

Since $d[r_1(\bar{r}_2 \cdot \bar{r}_1)]$ is an exact differential it does not contribute to the integral, so

$$\bar{A}(\bar{r}_2) = \frac{\mu_0 I}{4\pi}\left\{\frac{1}{r_2{}^3}\oint\frac{1}{2}(\bar{r}_1 \times d\bar{r}_1) \times \bar{r}_2\right\},$$

(2-60)

or

$$\bar{A}(\bar{r}_2) = \frac{\mu_0}{4\pi}\left\{\frac{I}{2}\oint\bar{r}_1 \times d\bar{r}_1\right\} \times \frac{\bar{r}_2}{r_2{}^3}.$$

(2-61)

The bracketed part of Equation 2-61 is defined as the magnetic dipole moment, $\bar{m}$.

Therefore Equation 2-61 can be rewritten as

$$\bar{A}(\bar{r}_2) = \frac{\mu_0}{4\pi}\frac{\bar{m} \times \bar{r}_2}{r_2{}^3}.$$

(2-62)

Now we have an expression for the vector potential of a current carrying loop at distances much greater than the dimensions of the loop. From this vector potential we can find the magnetic field by noting that

$$\bar{B}(r_2) = \bar{\nabla} \times \bar{A}(r_2) \,. \tag{2-63}$$

Substituting Equation 2-62 into 2-63 we get

$$\bar{B}(r_2) = \frac{\mu_0}{4\pi} \bar{\nabla} \times \left(\bar{m} \times \frac{\bar{r}_2}{r_2^3} \right) \,. \tag{2-64}$$

Applying the vector identity,

$$\nabla \times (\bar{X} \times \bar{Y}) = (\nabla \cdot \bar{Y})\bar{X} - (\nabla \cdot \bar{X})\bar{Y} + (\bar{Y} \cdot \nabla)\bar{X} - (\bar{X} \cdot \nabla)\bar{Y} \,, \tag{2-65}$$

to Equation 2-64 gives

$$\bar{B}(r_2) = \frac{\mu_0}{4\pi} \left[\left(\bar{\nabla} \cdot \frac{\bar{r}_2}{r_2^3} \right)\bar{m} - (\bar{\nabla} \cdot \bar{m})\frac{\bar{r}_2}{r_2^3} + \left(\frac{\bar{r}_2}{r_2^3} \cdot \bar{\nabla} \right)\bar{m} - (\bar{m} \cdot \bar{\nabla})\frac{\bar{r}_2}{r_2^3} \right] \,. \tag{2-66}$$

The magnetic dipole moment is a property of the magnetic field source and is, in this case, constant at the POC. Therefore, the derivatives of $\bar{m}$ in Equation 2-66 are zero. This leaves

$$\vec{B}(r_2) = \frac{\mu_0}{4\pi}\left[-(\vec{m}\cdot\vec{\nabla})\frac{\vec{r}_2}{r_2^{\;3}} + \vec{m}\left(\vec{\nabla}\cdot\frac{\vec{r}_2}{r_2^{\;3}}\right)\right].$$ (2-67)

By utilizing the fact that

$$m_x\frac{\partial}{\partial x_2} = \frac{m_x\hat{i}}{r_2^{\;3}} - 3m_x x_2\frac{\vec{r}_2}{r_2^{\;5}},$$ (2-68)

the first bracketed term in Equation 2-67 can be transformed into

$$(\vec{m}\cdot\vec{\nabla})\frac{\vec{r}_2}{r_2^{\;3}} = \frac{\vec{m}}{r_2^{\;3}} - \frac{3(\vec{m}\cdot\vec{r}_2)\vec{r}_2}{r_2^{\;5}}.$$ (2-69)

The second term is

$$\vec{m}\left(\vec{\nabla}\cdot\frac{\vec{r}_2}{r_2^{\;3}}\right) = \vec{m}\left[\frac{3}{r_2^{\;3}} - \vec{r}_2\cdot\frac{3\vec{r}_2}{r_2^{\;5}}\right] = 0.$$ (2-70)

That leaves

$$\vec{B}(r_2) = \frac{\mu_0}{4\pi}\left[-\frac{\vec{m}}{r_2^{\;3}} + \frac{3(\vec{m}\cdot\vec{r}_2)\vec{r}_2}{r_2^{\;5}}\right].$$ (2-71)

Equation 2-71 shows the magnetic field of a distant current-carrying loop. It depends only on the magnetic dipole moment of the loop.

To use Equation 2-71 to find the magnetic field of a circular loop it is necessary to find the magnetic moment of a circular loop. This calculation is fairly simple for a circular loop. The magnetic dipole moment is defined as

$$\bar{m} = I\bar{A}$$

(2-72)

where $\bar{A}$ in Equation 2-72 is NOT the vector potential. $\bar{A}$ is the area vector of the circular loop. For a circular loop

$$|\bar{m}| = I\pi r_1^2 \hat{n}$$

(2-73)

where r_1 is the radius of the circular loop and $\hat{n}$ is a unit vector parallel to the area vector $(\bar{A})$.

If we combine equation 2-71 and Equation 2-73 we get an equation for the magnetic field far away from a circular loop of wire:

$$\bar{B}(r_2) = \frac{\mu_0}{4\pi}\left[-\frac{I\pi r_1^2 \hat{n}}{r_2^3} + \frac{3I\pi r_1^2 (\hat{n}\cdot\bar{r}_2)\bar{r}_2}{r_2^5}\right].$$

(2-74)

To test the validity of this approximation we can compare the results for Equation 2-74 in the case of the POC being on the axis of a circular loop to the expected analytic result of Equation 2-42:

$$\bar{B}(r_2) = \frac{\mu_0 I}{2}\frac{(a^2)}{(a^2+z^2)^{3/2}}\hat{k}.$$

(2-42)

First, rewrite Equation 2-74, factoring out the constants and confining the geometry to match the geometry defined in Equation 2-42 ($r_1 = a$, $\hat{n} = \hat{k}$):

$$\bar{B}(r_2) = \frac{\mu_0 I}{4}\left[-\frac{a^2 \hat{k}}{r_2^{\ 3}} + \frac{3a^2\left(\hat{k}\cdot\vec{r}_2\right)\vec{r}_2}{r_2^{\ 5}}\right].$$

(2-75)

Combining the bracketed terms and simplifying where necessary we get

$$\bar{B}(r_2) = \frac{\mu_0 I}{2}\left[\frac{a^2 \hat{k}}{r_2^{\ 3}}\right],$$

(2-76a)

or

$$\bar{B}(z) \approx \frac{\mu_0 I}{2}\left[\frac{a^2 \hat{k}}{z^3}\right].$$

(2-76b)

Does this result match Equation 2-42? The major assumption in this approximation is that $r_2 \gg r_1$ ($z \gg a$). If we apply this assumption to Equation 2-42, we can obtain the same result. Start with Equation 2-42:

$$\bar{B}(r_2) = \frac{\mu_0 I}{2}\frac{\left(a^2\right)}{\left(a^2 + z^2\right)^{3/2}}\hat{k}.$$

(2-42)

Since $z \gg a$, we can rewrite Equation 2-42 as,

$$\bar{B}(r_2) \approx \frac{\mu_0 I}{2} \frac{\left(a^2\right)}{\left(z^2\right)^{\frac{3}{2}}} \hat{k} \qquad (2\text{-}77)$$

which simplifies to Equation 2-76b,

$$\bar{B}(z) \approx \frac{\mu_0 I}{2} \left[\frac{a^2 \hat{k}}{z^3} \right]. \qquad (2\text{-}76b)$$

So, yes Equation 2-75 is a valid approximation of the magnetic field at large distances away from the source loop.

Chapter 3

Results

In this chapter, the results of the calculation described in the previous chapter will be presented and analyzed. All calculations were performed using a variation of the MATLAB code listed in Chapter 2. The approximation of the field will be tested both qualitatively and analytically. For the analytical evaluation there are three areas in which this approximation can be examined. Those areas are: on the axis of the loop, near the axis of the loop, and the field "far" outside the loop.

With all the possible variations of the approximation, there are many parameters that are user controlled. The basic parameters are: the current, the number of turns in the loop, the number of sides in the polygon, the "radius" (the distance from the center of the polygon to each vertex), and the position(s) of the POC. The main difference in all the approximations is related to the POC. There are four basic variations of the basic Matlab program. Each variation has a specific way in which it allows the user to vary the parameters. Variation 1 allows the user to input the exact location of the POC, but it only calculates the magnetic field at that one point. Variations 2, 3 and 4 create three maps of the magnetic field, one for each of the components (r, θ, and z). The maps from second variation show the magnetic field in a plane parallel to the x-y plane at a user defined z-coordinate. The maps in the third variation show the magnetic field in a plane parallel to the y-z plane at a user defined x-coordinate. The maps for the fourth variation shows the field in the x-z plane at a user defined y-coordinate.

Variations 2, 3 and 4 output three graphs, one for each component, in cylindrical coordinates, of the magnetic field. For qualitatively checking the output of these

programs, the r- and z-components appear quite accurate for any number of sides higher than twenty-five. It is more useful to look at the θ-component of the magnetic field as the number of sides increases.

In a plane just above the polygonal loop the θ-component of the magnetic field should go to zero as the number of sides increases. This is evident in Figures 9b-15b. In Figure 15b (just above a 200-sided polygon) the θ-component is very close to zero. In fact, as n increases the θ-component becomes so small that all that is visible in the map in Figure 15b are numerical artifacts caused by a loss of precision when adding each side's contribution to the magnetic field. However, the actual magnitude of the θ-component of the magnetic field in these areas is on the order of at least 10^{-5} times less than the magnitude of the other components of the magnetic field so the θ-component of the magnetic field is essentially negligible. This fact gives good evidence that it is reasonable to use a polygon to approximate the magnetic field.

As a further check on the accuracy, the axial field of the approximation was compared to the analytic solution of the Biot-Savart law for a circular loop. This check produced some interesting results.

It was originally expected that, as z increased, the axial field of the polygon would approach that of the circular loop. This, however, is not the case. The percent error in the field, as z increased, approached a constant rather than zero (Figure 16). As it turns out, this error is related to the difference in the area between the polygon and the circle. This matches the results from Reitz, et. al. p 210. For large distances, the magnetic field approximately matches the magnetic field of a magnetic dipole. The magnetic field of a dipole depends only on the current and the area of the loop.

An interesting observation, resulting from the error analysis of the axial field, was that for z values much greater than the radius of the polygonal loop the percent error decreased proportionally with $\frac{1}{n^2}$ (Figure 17). This decrease in the error corresponds to the difference in the areas between the polygon and the circle. The difference in the areas between a circle and a polygon decreases as $\frac{1}{n^2}$.

One result that came out of the error analysis was that for any finite number of sides to the polygon there were two points (spaced symmetrically around the loop) that yield a percent error of zero. For z smaller than that value the field is overestimated. For z larger than that point the field is underestimated. For an inscribed polygon, the points of the loop are closer to the axis than the points along a circular loop. For all points on the axis the magnitude of the field produced by a part of the polygonal loop is greater. The direction, however, is slightly different. At small z, the magnitude of the field for the polygon wins out over the one for the circular loop. At large z, the field of a polygonal loop is more horizontal than that of the circle. This means that the vertical component of the field for the circle is greater than that of the polygon, so the polygonal approximation is less than the actual magnetic field.

This point of zero error (PZE) is limited (Figure 18). As the number of sides increases, the PZE approaches a value of $\frac{\sqrt{2}}{2} \approx 0.707$. By graphing the point of zero error vs. n and using the graphical analysis abilities in LoggerPro, the PZE approaches its value as $\frac{1.5}{n^2}$. This result, while interesting, doesn't reveal much since the error in the magnetic field goes to zero at the same rate that the PZE approaches $\frac{\sqrt{2}}{2} \approx 0.707$.

Another test for the polygonal approximation is to compare it to the near axis approximation. As shown in the previous chapter, the r-component of the magnetic field near the axis of a circular current carrying loop is:

$$B_r \approx \frac{3\mu_0 I}{4} \frac{azr}{\left(z^2 + a^2\right)^{5/2}}.$$ (2-51)

For $n = 200$ the polygonal approximation matches this linear approximation for the radial component of the field to within less than 10 percent for r values less 0.23m with a 1m radius loop at z=0.1m (Figure 19).

The linear approximation for the radial component is only meant to work for values of r that are much smaller than the radius of the current carrying loop. Using r=0.23m in the linear approximation with a=1m is pushing the limits of the approximation; however, the percent difference between the linear approximation and the polygonal approximation gives a good indication of the value of the polygonal approximation for calculating the magnetic field of a circular loop.

Another indication that the polygonal approximation is valid is to look at the difference between the radial component of the polygonal approximation and the linear approximation. The graph of this difference versus radial position consists of the higher order terms in the series used to develop the linear approximation:

$$B_r = c_0 + c_1 r + c_2 r^2 + c_3 r^3 + ...$$ (2-48)

In fact, the graph of the difference versus radial position is mostly the cubic term of this series.

The final test of the reliability of the polygonal approximation is to look at the field far from the loop by comparing it to the magnetic dipole approximation for a circular loop of wire:

$$\bar{B}(r_2) = \frac{\mu_0}{4\pi}\left[-\frac{I\pi r_1^2 \hat{n}}{r_2^3} + \frac{3I\pi r_1^2 (\hat{n}\cdot\bar{r}_2)\bar{r}_2}{r_2^5} \right].$$

(2-74)

As seen with the axial field, the percent difference between the polygonal approximation and the dipole approximation goes to a constant value as the distance from the loop increases (Figure 20). The value of the percent difference is equal to the percent difference in the area of a circle compared to that of the approximating polygonal loop. Also as the number of sides (n) in the polygon increases the percent error decreases approximately as $1/n^2$. This is expected since at large distances the area plays the predominant role in the magnitude of the field produced by a current carrying loop, and the percent difference in the area of a circle compared to that of an inscribed polygon goes as $1/n^2$.

Chapter 4

Conclusions

The Biot-Savart law cannot be solved analytically at all points in space for a circular loop of wire. The only place where the Biot-Savart law can be solved is on the axis of the loop. For all other points in space it can only be approximated. One way in which this is done is to approximate the circular loop as a many-sided regular polygon and solving the Biot-Savart law directly for each side. The magnetic field for the loop is then the vector sum of the contributions of each side.

To do this approximation manually is computationally intensive. To reduce the effort required to perform this approximation, it is feasible to automate the process in MATLAB. Automating the magnetic field approximation also allows for easily mapping the magnetic field.

By its nature, the magnetic fields are difficult to visualize. Having a program that can map the magnetic field can be an invaluable asset. Having a map of the magnetic field allows a person see how each component of the magnetic field varies with position.

There are limitations to the programs discussed here. The first limitation is that they only map the magnetic field one plane at a time. For each version of the program one component of the position is kept constant. This is done for a couple of reasons to shorten the runtime of the program and, more importantly, if one component of the position is kept constant when the magnetic field is mapped it frees up one axis of the graph to be used to show the magnitude of the field.

Time is another limitation of the programs. Automating the calculations certainly cuts down the amount of time it takes to get results compared to running through the calculations by hand, but it is still an issue, especially in the case where maps of the magnetic field are created. For a 200-sided polygon a map consisting of a 200 x 200 square grid, it still takes about twenty-four hours for the simulation to make all the calculations and return results on a Dell Optiplex GX280 with a 2.80 GHz Pentium 4 and 1 GB of RAM.

For all the results, the polygon that was used to approximate the circular loop was inscribed in a circle that matched the circular loop. What if, instead of inscribing the polygon, it is circumscribed around the circular loop? The result of this condition is that the error in the axial field is reduced to approximately half of the inscribed loop. As expected the error also decreases no slower than $\frac{1}{n^2}$.

Using an inscribed polygon overestimates the magnetic field close to the loop and underestimates the magnetic field far away. A circumscribed polygon does just the opposite. It underestimates the field close and overestimates far away. Given that the error for a circumscribed polygon goes to half the value of the error of an inscribed polygon as z approaches infinity, it may be useful to combine these approximations with a weighted average to approximate the magnetic field. The usefulness of this is that it will reduce the error at the far limit to zero. It will also reduce the error near the loop on the axis. A disadvantage of using a weighted average is that it increases the space around the loop where the approximation is not valid. However, for a sufficiently large number of sides, this space is only negligibly larger than either of the individual approximations. Another disadvantage of using this weighted average is that it doubles the already lengthy

calculation time and since, for large n, the inscribed polygonal approximation is really close to the actual axial magnetic field, reducing the time of calculation is more advantageous than decreasing an already small error.

Appendix A

Derivation of Ampere's law from the law of Biot and Savart

Ampere's law is derived from the Biot-Savart law by first assuming that there is a

steady current. That is to say,

$$\bar{\nabla} \cdot \bar{J} = 0. \tag{A-4}$$

Then take the curl with respect to $\bar{r}_2$ of both sides of the Biot-Savart law:

$$\bar{\nabla}_2 \times \bar{B}(\bar{r}_2) = \bar{\nabla}_2 \times \left[\frac{\mu}{4\pi} \oint \frac{\bar{J}(\bar{r}_1) \times (\bar{r}_2 - \bar{r}_1)}{|\bar{r}_2 - \bar{r}_1|^3} dV \right]. \tag{A-5}$$

This becomes

$$\bar{\nabla}_2 \times \bar{B}(\bar{r}_2) = \frac{\mu}{4\pi} \int_V \left[\left(\bar{\nabla}_2 \cdot \frac{(\bar{r}_2 - \bar{r}_1)}{|\bar{r}_2 - \bar{r}_1|^3} \right) \bar{J} - \left(\bar{\nabla}_2 \cdot \bar{J} \right) \frac{(\bar{r}_2 - \bar{r}_1)}{|\bar{r}_2 - \bar{r}_1|^3} \right.$$

$$\left. + \left(\frac{(\bar{r}_2 - \bar{r}_1)}{|\bar{r}_2 - \bar{r}_1|^3} \cdot \bar{\nabla}_2 \right) \bar{J} - \left(\bar{J} \cdot \bar{\nabla}_2 \right) \left(\frac{(\bar{r}_2 - \bar{r}_1)}{|\bar{r}_2 - \bar{r}_1|^3} \right) \right] dV. \tag{A-6}$$

The second term of equation (1-6) is zero due to equation (1-4). The third term of

equation (1-6) is zero because the derivative is taken with respect to $\bar{r}_2$, and $\bar{J}(\bar{r})$ is only

a function of $\bar{r}_1$. Equation (1-6) then becomes

$$\vec{\nabla}_2 \times \vec{B}(\vec{r}_2) = \frac{\mu}{4\pi} \int_V \left[\left(\vec{\nabla}_2 \cdot \frac{(\vec{r}_2 - \vec{r}_1)}{|\vec{r}_2 - \vec{r}_1|^3} \right) \vec{J} - \left(\vec{J} \cdot \vec{\nabla}_2 \right) \left(\frac{(\vec{r}_2 - \vec{r}_1)}{|\vec{r}_2 - \vec{r}_1|^3} \right) \right] dV . \qquad \text{(A-7)}$$

Now make the following changes. Express the first term as a Dirac delta function. Multiply the second term by negative one and change the derivative to differentiate with respect to $\vec{r}_1$:

$$\vec{\nabla}_2 \times \vec{B}(\vec{r}_2) = \frac{\mu}{4\pi} \int_V \left[4\pi \cdot \vec{J} \delta(\vec{r}_2 - \vec{r}_1) - \left(\vec{J} \cdot \vec{\nabla}_1 \right) \left(\frac{(\vec{r}_1 - \vec{r}_2)}{|\vec{r}_2 - \vec{r}_1|^3} \right) \right] dV . \qquad \text{(A-8)}$$

The first term here integrates immediately to $4\pi \, \vec{J}$. The second term of this equation is zero (Reitz et al 204).

We can use the following vector identity to show that the second term of equation (1-8) is zero. For the x-component of $\vec{r}_1$ and $\vec{r}_2$,

$$\vec{\nabla}_1 \cdot \left(\vec{J} \frac{(x_1 - x_2)}{|\vec{r}_2 - \vec{r}_1|^3} \right) = \frac{(x_1 - x_2)}{|\vec{r}_2 - \vec{r}_1|^3} \vec{\nabla}_1 \cdot \vec{J} + \left(\vec{J} \cdot \vec{\nabla}_1 \right) \left(\frac{(x_1 - x_2)}{|\vec{r}_2 - \vec{r}_1|^3} \right) . \qquad \text{(A-9)}$$

$\vec{\nabla} \cdot \vec{J} = 0$. So,

$$\left(\vec{J} \cdot \vec{\nabla}_1 \right) \left(\frac{(x_1 - x_2)}{|\vec{r}_2 - \vec{r}_1|^3} \right) = \vec{\nabla}_1 \cdot \left(\vec{J} \frac{(x_1 - x_2)}{|\vec{r}_2 - \vec{r}_1|^3} \right) . \qquad \text{(A-10)}$$

Substitute this into equation (1-8) to yield

$$\bar{\nabla}_2 \times \bar{B}(\bar{r}_2) = \mu_0 \bar{J} - \int_V \bar{\nabla}_1 \cdot \left(\bar{J} \frac{(x_1 - x_2)}{\left| \bar{r}_2 - \bar{r}_1 \right|^3} \right) dV. \qquad \text{(A-11)}$$

Now we can use the divergence theorem on this integral:

$$\bar{\nabla}_2 \times \bar{B}(\bar{r}_2) = \mu_0 \bar{J} - \oint_S \frac{(x_1 - x_2)}{\left| \bar{r}_2 - \bar{r}_1 \right|^3} \bar{J} \cdot d\bar{a}. \qquad \text{(A-12)}$$

The surface integral corresponds to the normal component of $\bar{J}$. Therefore this term must be zero. If this integral were not zero, there would be a net flow of current out of the region (Cook 141). Equations A-9 through A-12 can be repeated for the y- and z-components with the same results, so we end up with

$$\bar{\nabla}_2 \times \bar{B}(\bar{r}_2) = \mu_0 \bar{J}. \qquad \text{(A-13)}$$

This is normally referred to as Ampere's law before James Clerk Maxwell added in a term for the displacement current.

Sometimes it is useful to express Equation (1-13) in integral form. This can be done by integrating each side over a surface that crosses the path of the current. This surface is referred to as an Amperian surface

$$\int_S \bar{\nabla} \times \bar{B} \cdot d\bar{A} = \mu_0 \int_S \bar{J} \cdot d\bar{A} \qquad \text{(A-14)}$$

where $d\bar{A}$ is a vector in the direction normal to the surface whose magnitude is a differential area of the Amperian surface.

Applying Stokes's theorem to the left side of this equation, we get

$$\int_S \bar{\nabla} \times \bar{B} \cdot d\bar{A} = \oint_C \bar{B} \cdot d\bar{l} \qquad \text{(A-15)}$$

where $d\bar{l}$ is a differential length along the perimeter of the Amperian surface. This changes a surface integral over an open surface into a path integral around a closed path.

Substituting equation (1-15) into equation (1-14), we get the integral for of Ampere's law:

$$\oint_C \bar{B} \cdot d\bar{l} = \mu_0 \int_S \bar{J} \cdot d\bar{A} . \qquad \text{(A-16)}$$

For a single wire, $\bar{J}$ is a constant so we can simplify the right side of equation A-16 to $\mu_0 I$. So, for a single wire the integral form of Ampere's law is

$$\oint_C \bar{B} \cdot d\bar{l} = \mu_0 I . \qquad \text{(A-17)}$$

Solving equation (A-17) for a long straight wire will yield the same result as in equation (A-1). This verifies that equation (A-3) and equation (A-13) are equivalent in that, though developed independently, they both yield the same result:

$$\left| \bar{B} \right| = \frac{\mu_0 I}{2\pi r} . \qquad \text{(A-18)}$$

References

Atkin, R. H. *Theoretical Electromagnetism.* New York: John Wiley & Sons, 1962.

Binns, K. J. and P. J. Lawrenson. *Analysis and Computation of Electric and Magnetic Field Problems.* New York: Macmillan, 1963.

Chase, Carl Trueblood. *A History of Experimental Physics.* New York: D. Van Nostrand Company, 1932.

Cook, David M. The Theory of the Electromagnetic Field. Englewood Cliffs, New Jersey: Prentice-Hall, 1975.

Corson, Dale and Paul Lorrain. Introduction to Electromagnetic Fields and Waves. San Francisco: W. H. Freeman and Company, 1962.

Griffiths, David J. Introduction to Electrodynamics. Englewood Cliffs, New Jersey: Prentice-Hall, Inc, 1981.

Grivich, Matthew I. and David P. Jackson. "The Magnetic Field of Current-carrying Polygons: An Application of Vector Field Rotations." *American Journal of Physics.* 68 (5), May 2000, 469-474.

Heilbron, J. L. Electricity in the Seventeenth and Eighteenth Centuries. Berkley: University of California Press, 1979.

Jackson, John David. Classical Electrodynamics. New York: John Wiley & Sons, 1975.

Knierim, Thomas. "Thales." Early Greek Philosophy. 26 July 2003. The Big View. 28 Sept 2003 http://www.thebigview.com/greeks/thales.html.

Lee, E.W. Magnetism: An Introductory Survey. New York: Dover Publications, Inc, 1970.

Meyer, Herbert W. A History of Electricity and Magnetism. Norwalk, Connecticut:

Burndy Library, 1972.

Panofsky, Wolfgang K. H., and Melba Phillips. <u>Classical Electricity and Magnetism</u>. Reading, Massechusetts: Addison-Wesley, 1962.

Purcell, Edward M. <u>Electricity and Magnetism</u>. New York: McGraw-Hill, 1965.

Reitz, John R., and Frederick J. Milford, and Robert W. Christy. Foundations of Electromagnetic Theory. Reading, Massechusetts: Addison-Wesley, 1993.

Serway, Raymond A. Physics for Scientists and Engineers. Philadelphia: Saunders, 1996.

Von Laue, Max. <u>History of Physics</u>. New York: Academic Press, 1950.

Weisstein[a], Eric. "Ampere, Andre (1775-1836)." <u>Eric Weisstein's World of Scietific Biography</u>. Wolfram Reasearch. 28 Sept 2003. http://scienceworld.wolfram. com/biography/Ampere.html.

---[b]. "Faraday, Michael (1791-1867)." <u>Eric Weisstein's World of Scietific Biography</u>. Wolfram Reasearch. 28 Sept 2003. http://scienceworld.wolfram. com/biography/Faraday.html.

---[c]. "Oersted, Hans (1777-1851)." <u>Eric Weisstein's World of Scietific Biography</u>. Wolfram Reasearch. 28 Sept 2003. http://scienceworld.wolfram. com/biography/Oersted.html.

Whitmer, Robert M. <u>Electromagnetics</u>. Englewood Cliffs, New Jersey: Prentice-Hall, Inc, 1962.
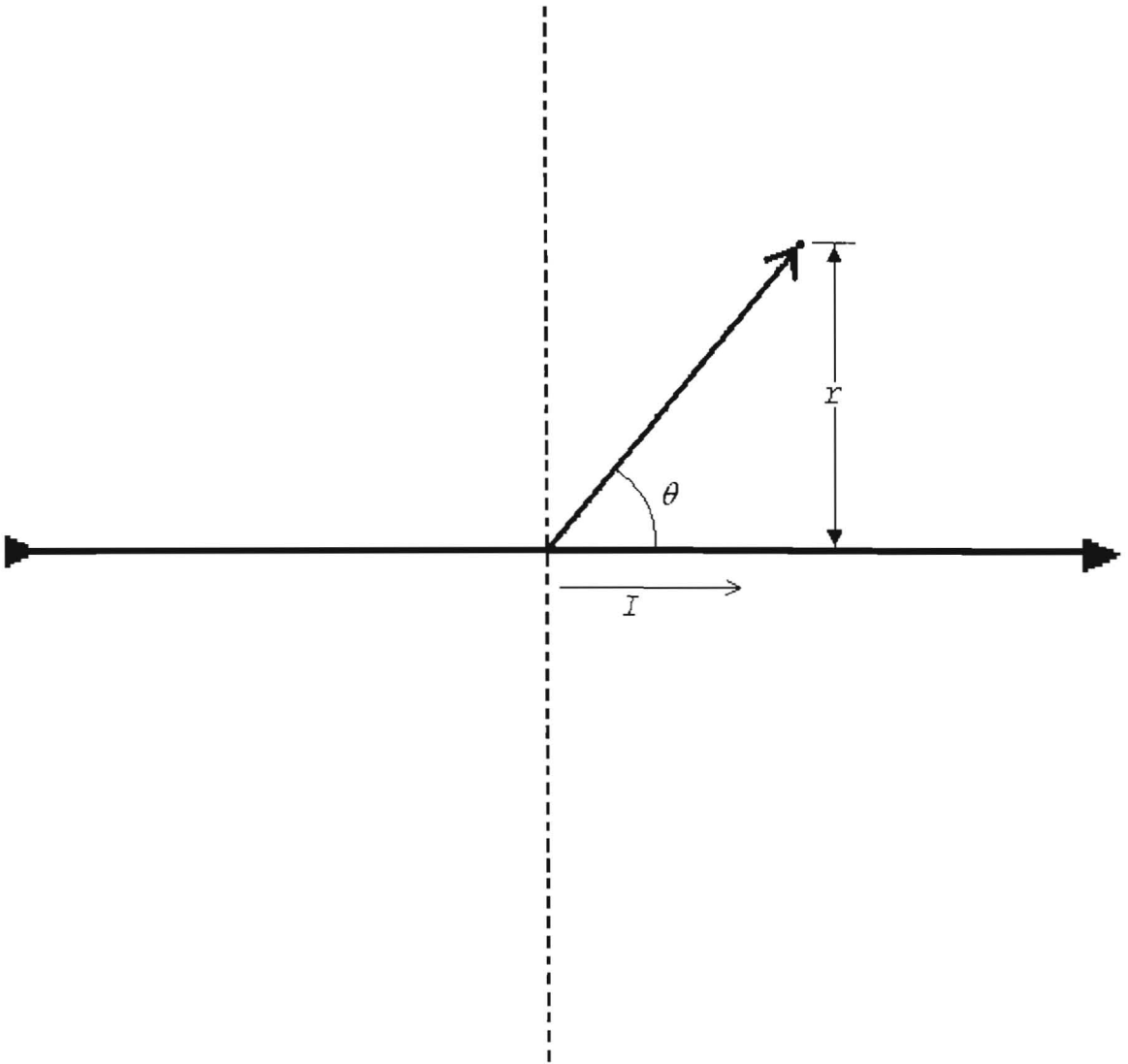
Figure 1. Diagram for the magnetic field of an infinitely long straight wire with current (I) at a distance (r) from the wire.
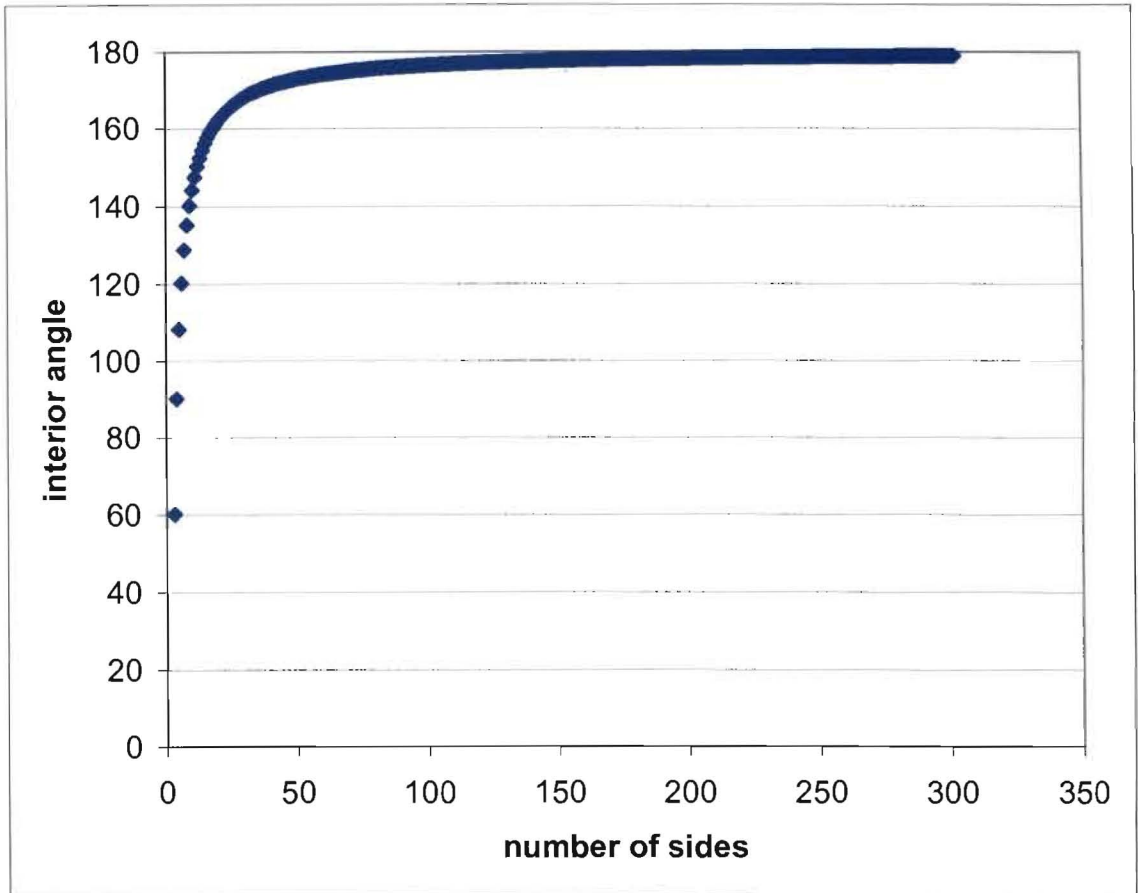
Figure 2. Graph of interior angles of a regular polygon as a function of the number of sides.

48
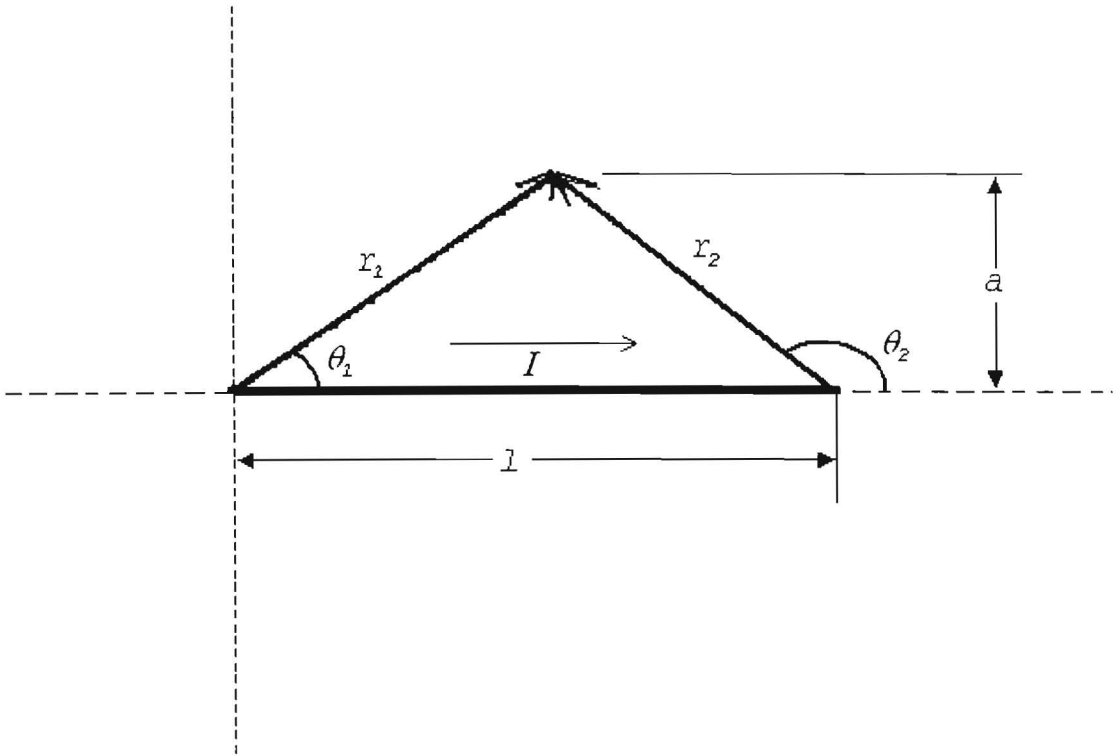
Figure 3. Diagram for the calculation of magnetic field for a straight wire segment.
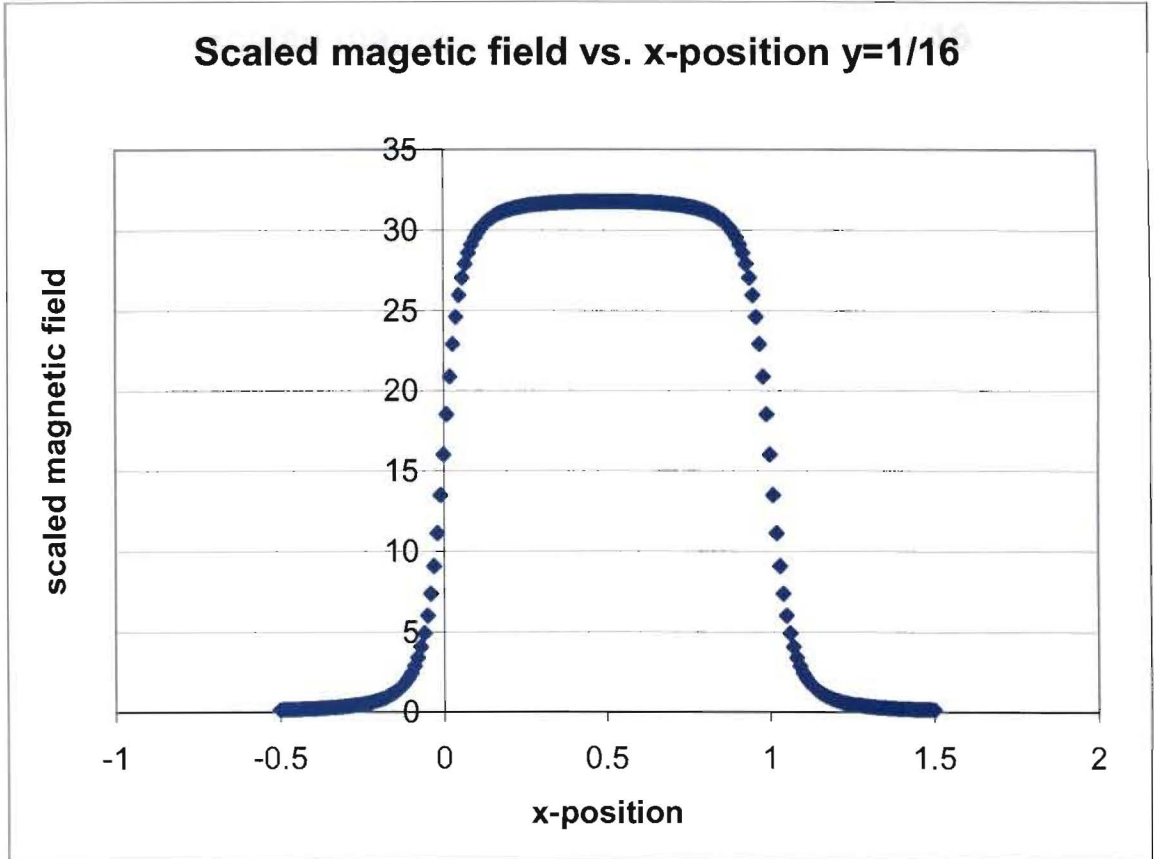
Figure 4. Graph showing the shape of the magnetic field (Equation 16) of a wire segment one meter in length as a function of horizontal position *x* keeping vertical position *y* positive and constant.
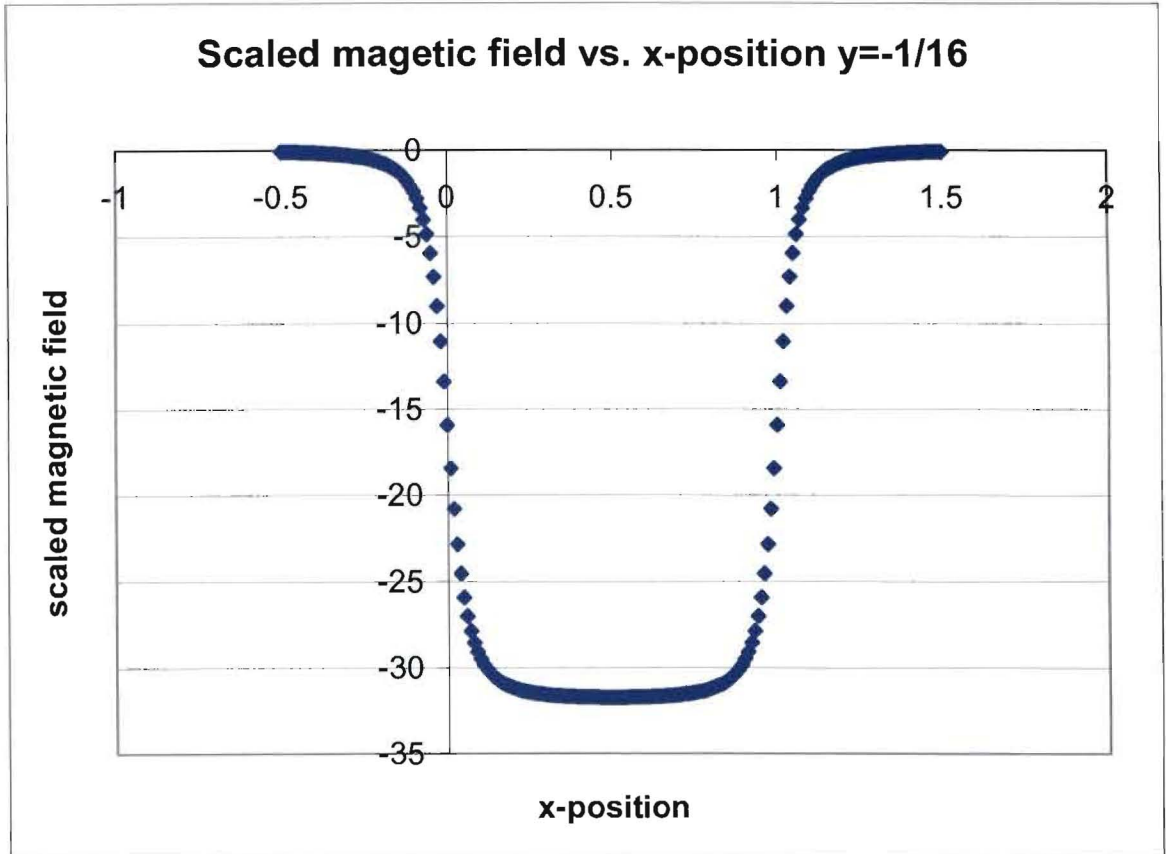
Figure 5. Graph showing the shape of the magnetic field (Equation 16) of a wire segment one meter in length as a function of horizontal position *x* keeping vertical position *y* negative and constant.
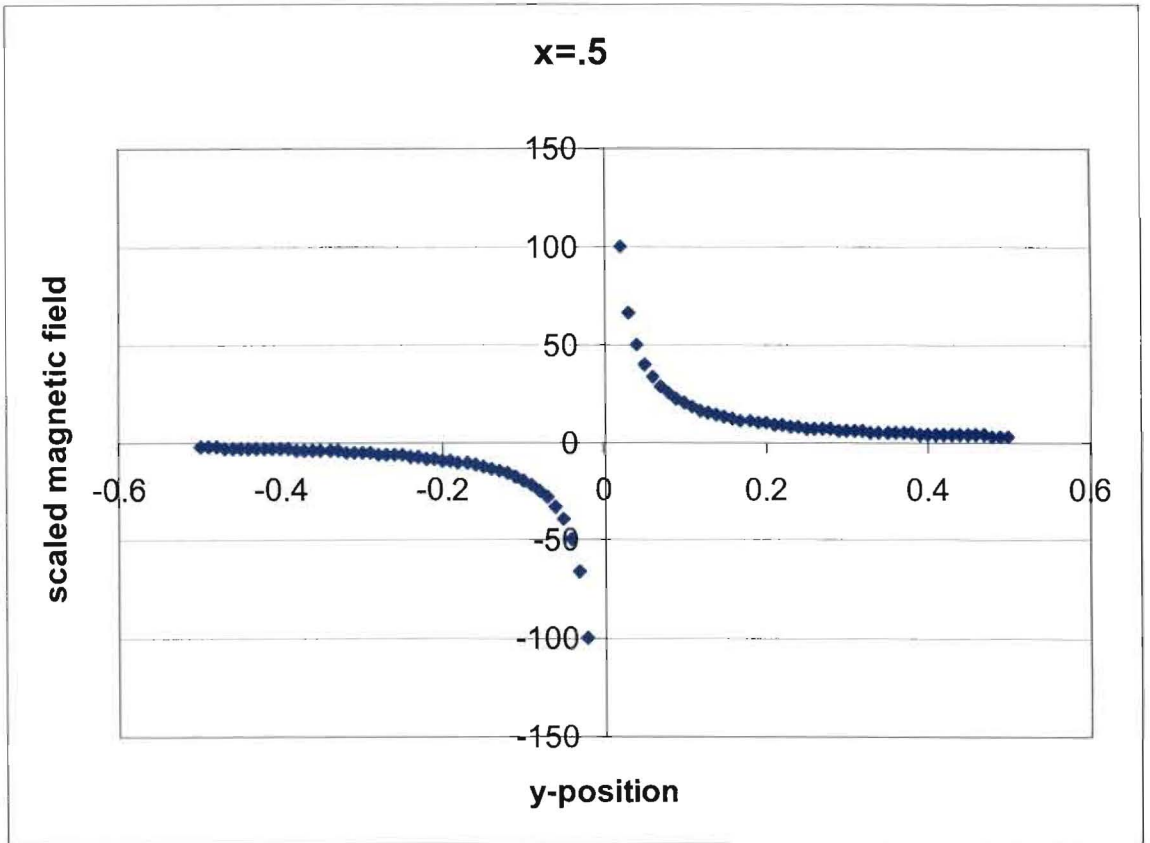
Figure 6. Graph showing the shape of the magnetic field (Equation 16) of a wire segment one meter in length as a function of vertical position *y* keeping horizontal position *x* constant and crossing the wire segment.
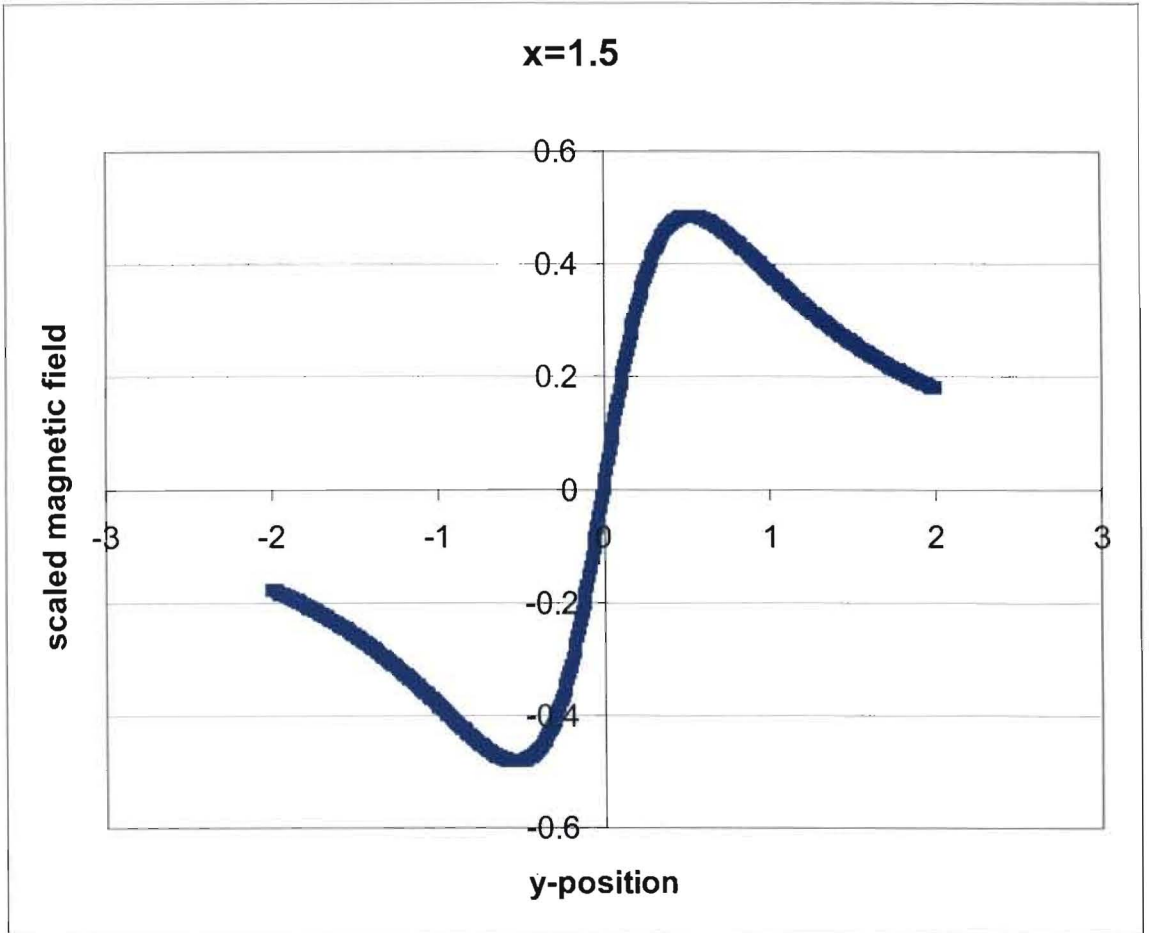
Figure 7. Graph showing the shape of the magnetic field (Equation 16) of a wire segment one meter in length as a function of vertical position y keeping horizontal position x constant and crossing the x-axis outside the wire segment.
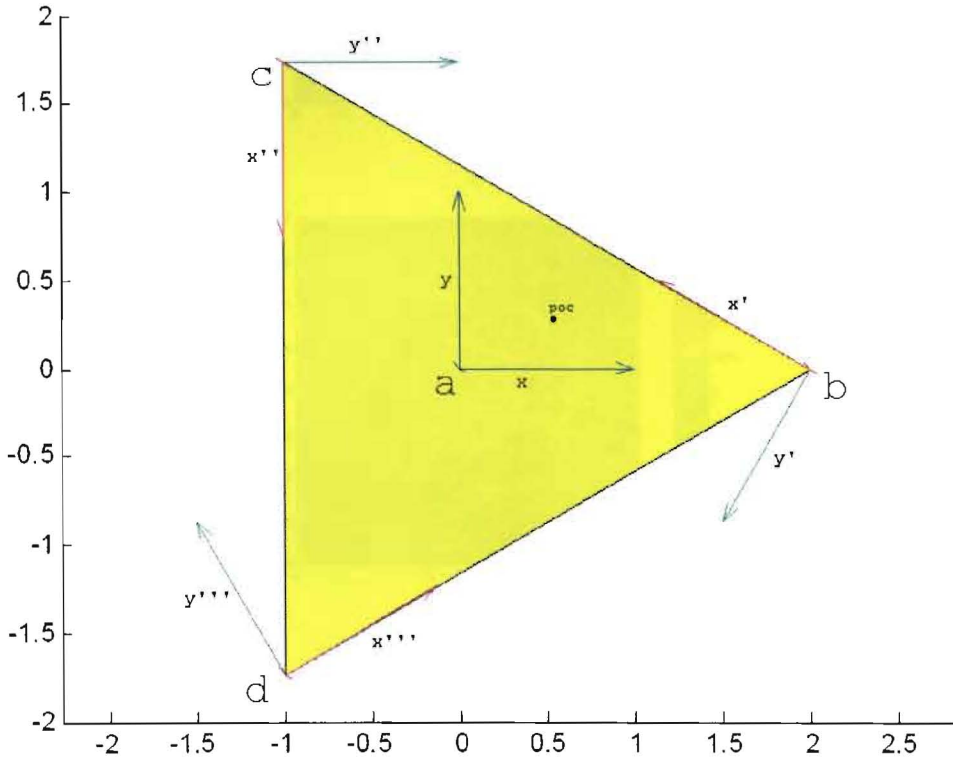
Figure 8. These four diagrams show the coordinate systems for a current carrying triangle. (a) The unprimed coordinate system. (b) The first primed coordinate system. (c) The second primed coordinate system. (d) The fourth and final coordinate system. In all cases, the z-direction is straight out of the page for the shown POC place in the x-y plane.
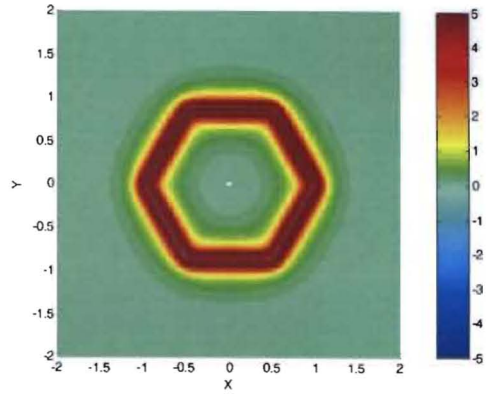
(a)
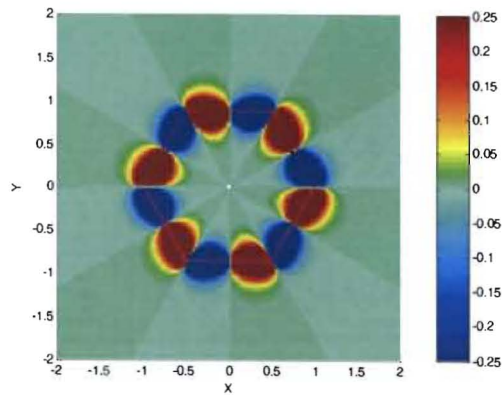
(b)
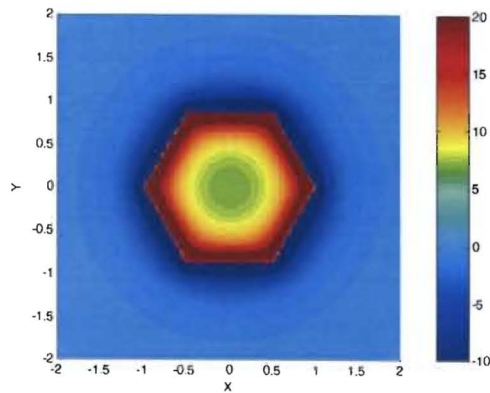
(c)

Figure 9. These show the magnitudes of each component of the magnetic field for a hexagon (1 m from center to vertex) as a function of position in cylindrical coordinates. (a) r-component vs. position. (b) θ-component vs. position. (c) z-component vs. position. For all of these graphs z=0.25m.
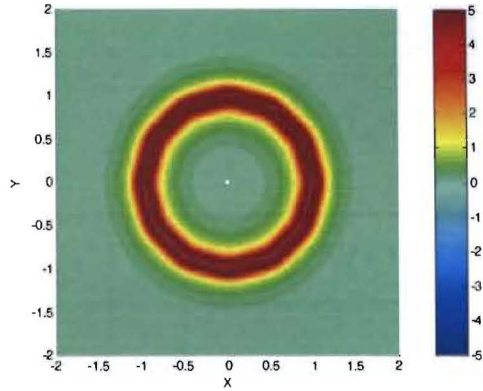
(a)
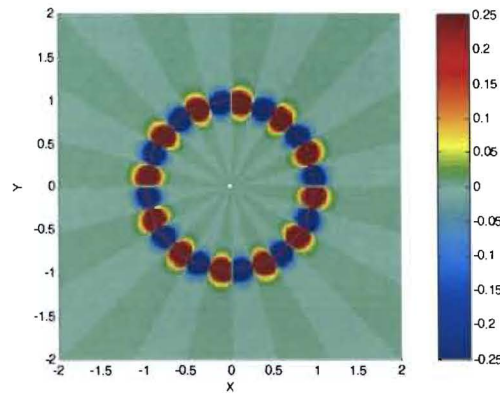
(b)
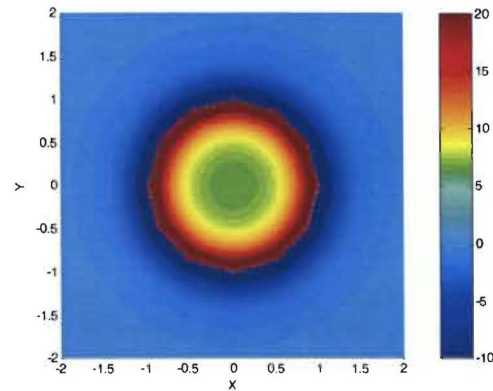
(c)

Figure 10. These show the magnitudes of each component of the magnetic field for a 12-sided polygon (1 m from center to vertex) as a function of position in cylindrical coordinates. (a) r-component vs. position. (b) θ-component vs. position. (c) z-component vs. position. For all of these graphs z=0.25m.
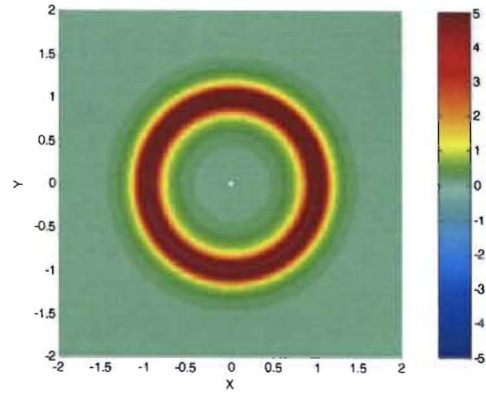
(a)
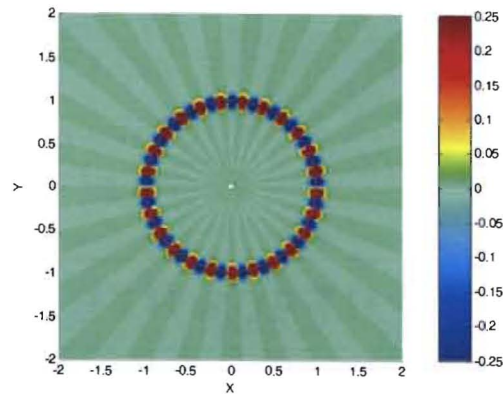
(b)
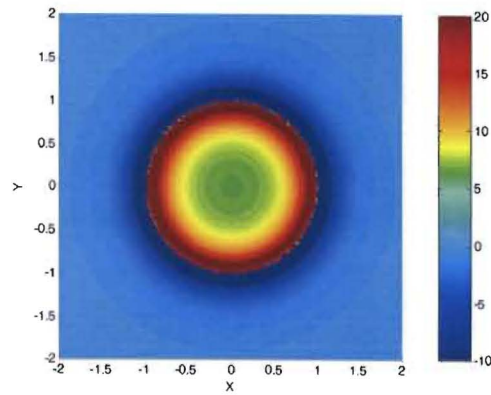
(c)

Figure 11. These show the magnitudes of each component of the magnetic field for a 25-sided polygon (1 m from center to vertex) as a function of position in cylindrical coordinates. (a) r-component vs. position. (b) θ-component vs. position. (c) z-component vs. position. For all of these graphs $z=0.25$m.
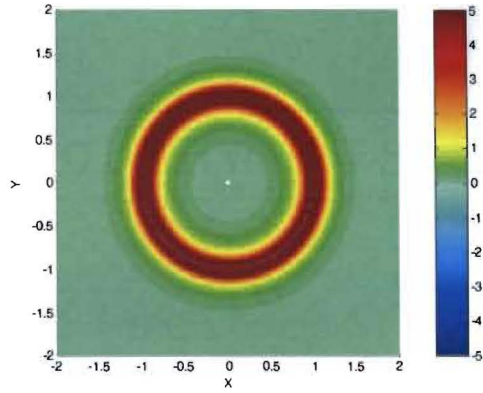
(a)
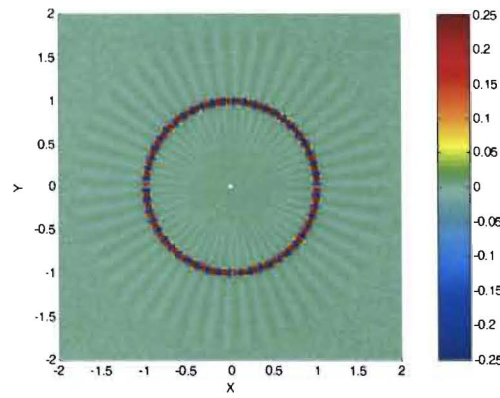
(b)
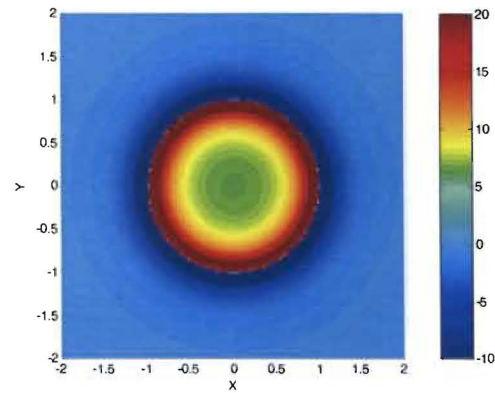
(c)

Figure 12. These show the magnitudes of each component of the magnetic field for a 50-sided polygon (1 m from center to vertex) as a function of position in cylindrical coordinates. (a) r-component vs. position. (b) θ-component vs. position. (c) z-component vs. position. For all of these graphs z=0.25m.
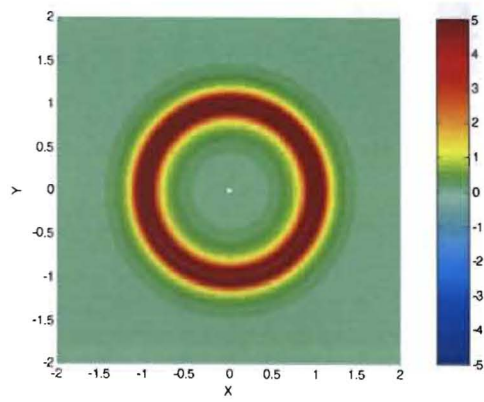
(a)
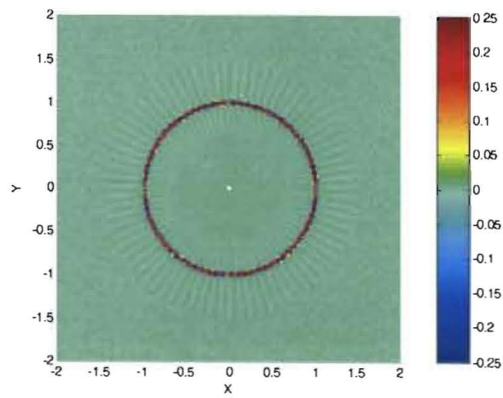
(b)
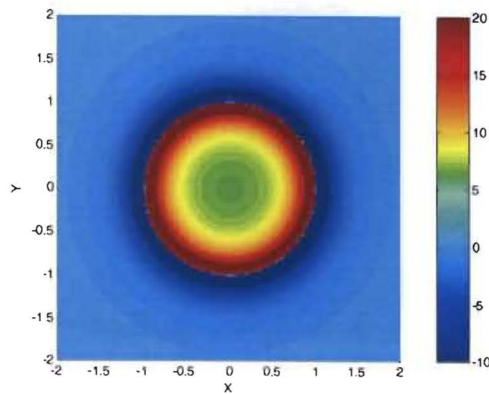
(c)

Figure 13. These show the magnitudes of each component of the magnetic field for a 75-sided polygon (1 m from center to vertex) as a function of position in cylindrical coordinates. (a) *r*-component vs. position. (b) *θ*-component vs. position. (c) *z*-component vs. position. For all of these graphs *z*=0.25m.
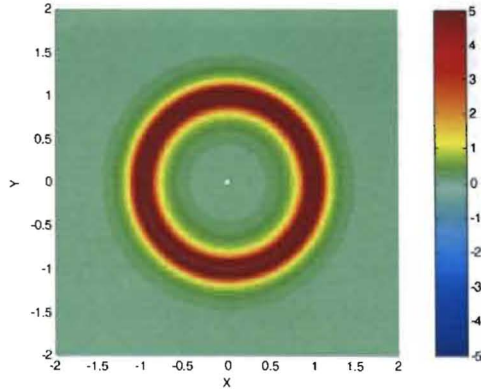
(a)
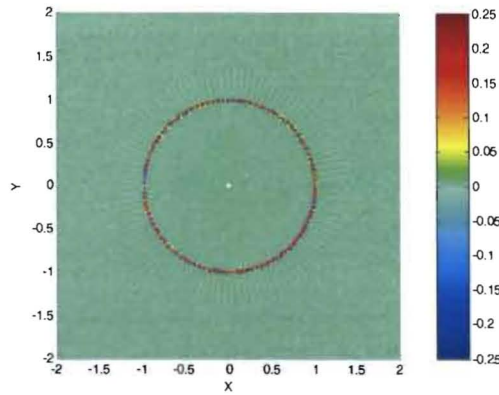
(b)
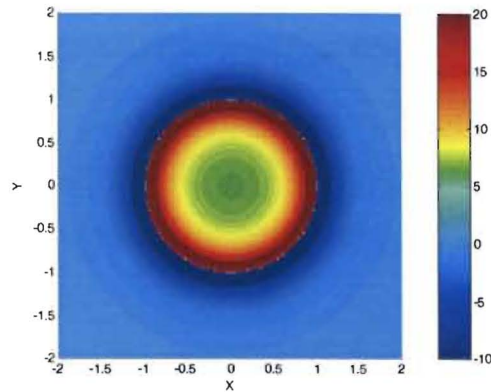
(c)

Figure 14. These show the magnitudes of each component of the magnetic field for a 100-sided polygon (1 m from center to vertex) as a function of position in cylindrical coordinates. (a) r-component vs. position. (b) θ-component vs. position. (c) z-component vs. position. For all of these graphs z=0.25m.

(a)

(b)

(c)
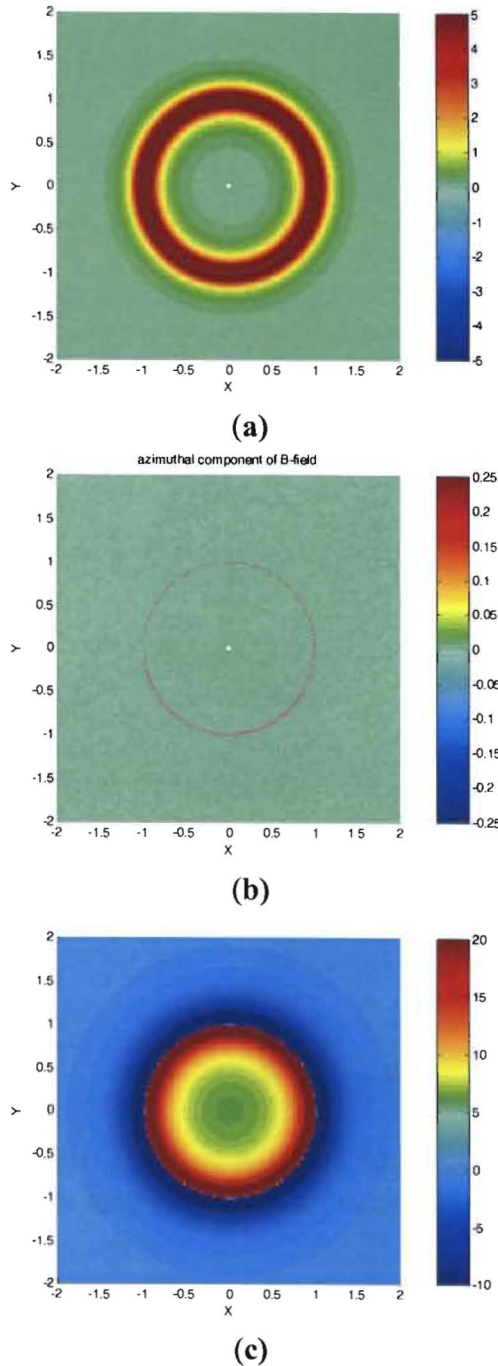
Figure 15. These show the magnitudes of each component of the magnetic field for a 200-sided polygon (1 m from center to vertex) as a function of position in cylindrical coordinates. (a) r-component vs. position. (b) θ-component vs. position. (c) z-component vs. position. For all of these graphs z=0.25m.
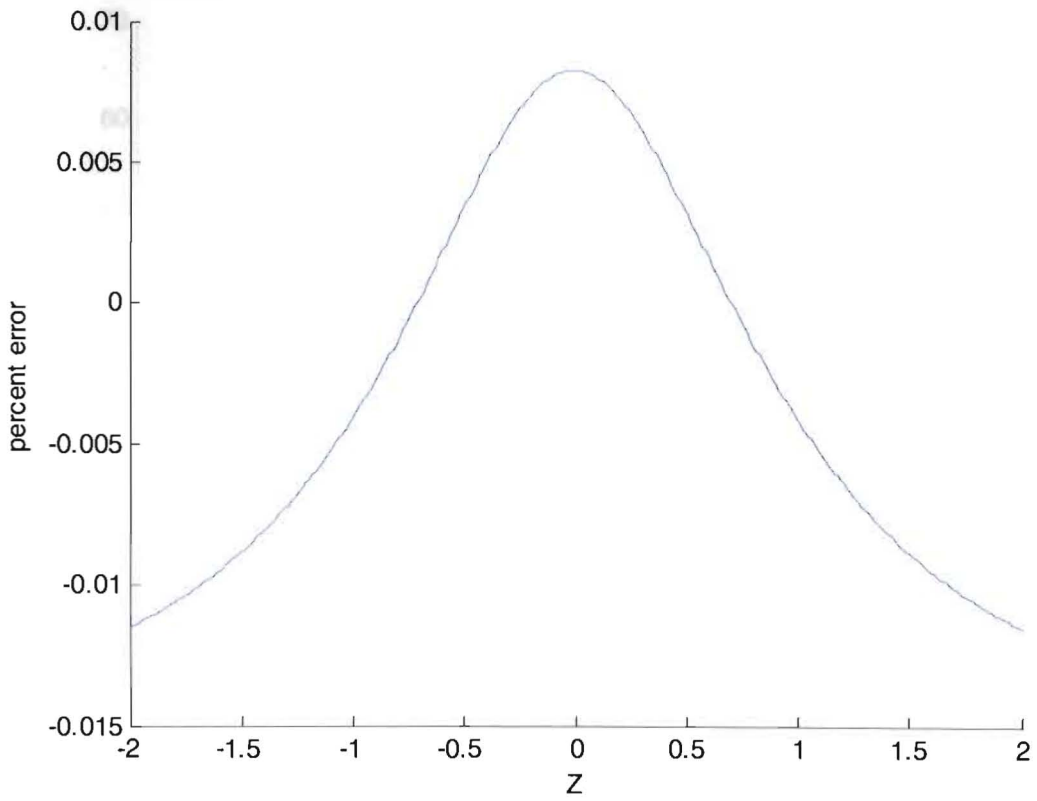
Figure 16. The percent error in the on-axis field of a 200-sided polygonal loop compared to the on-axis field of a circular loop graphed as a function of z.
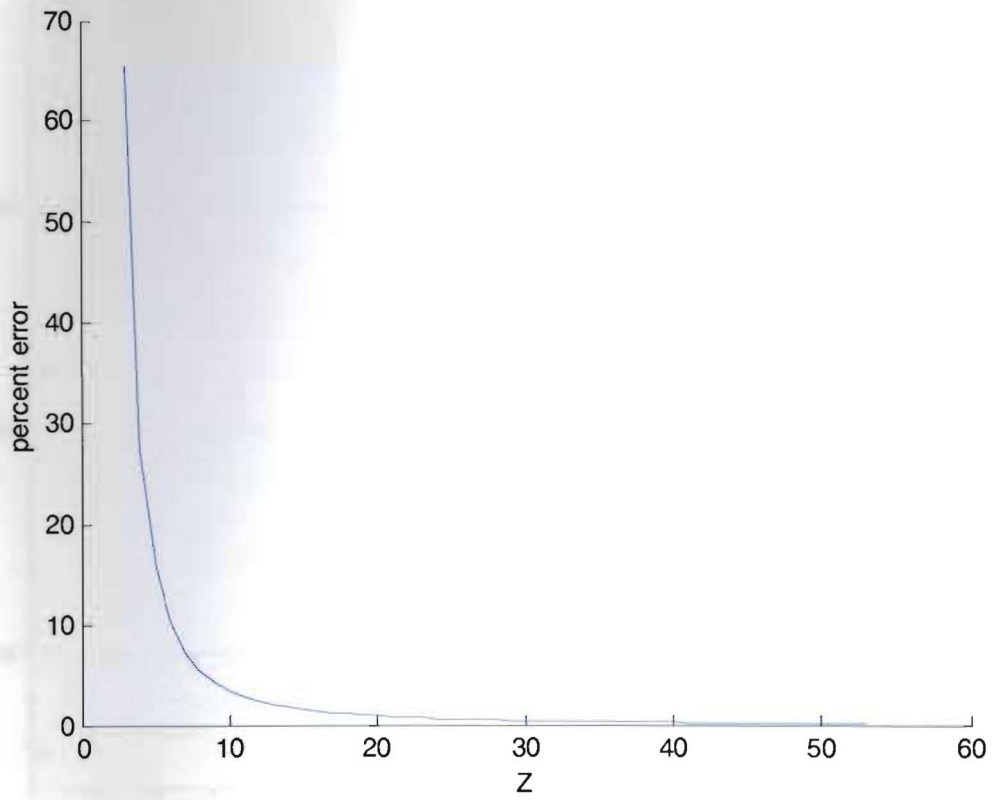
Figure 17. The percent error in the axial field of a polygonal loop at a fixed position $z=0$ graphed as a function of the number of sides (n).
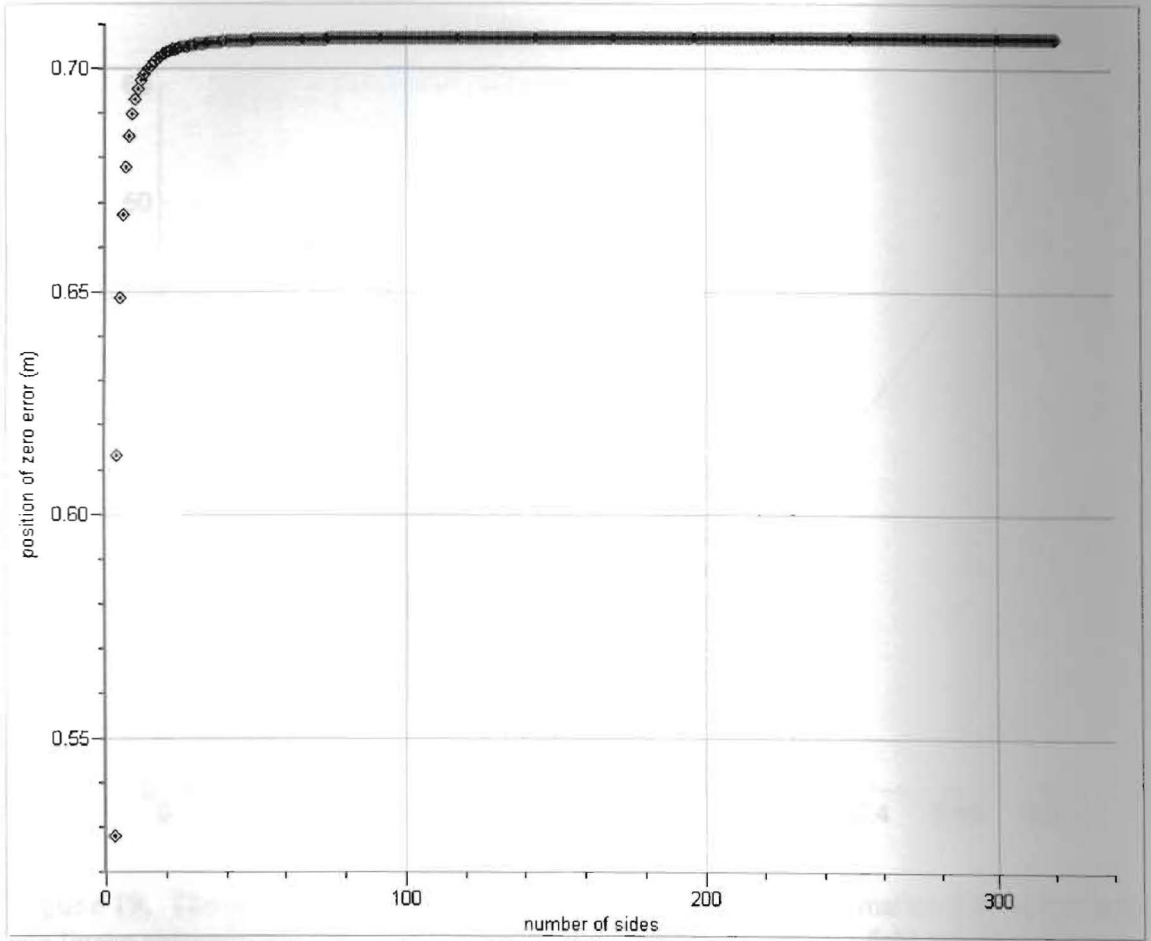
Figure 18. A graph showing the position of the point of zero error graphed as a function of the number of sides (*n*) in the polygonal loop.
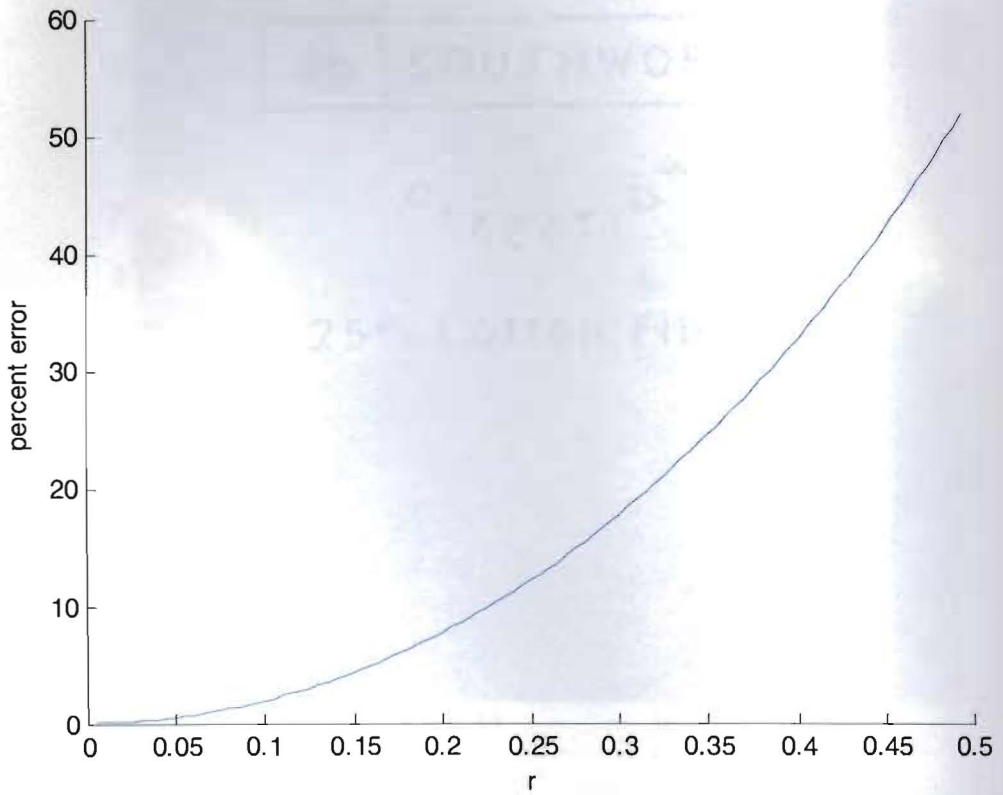
Figure 19. The percent difference between the polygonal approximation (200 sides) and the linear approximation for the radial component of the magnetic field graphed as a function of the distance from the axis of the loop (*r*) at *z*=0.01m.
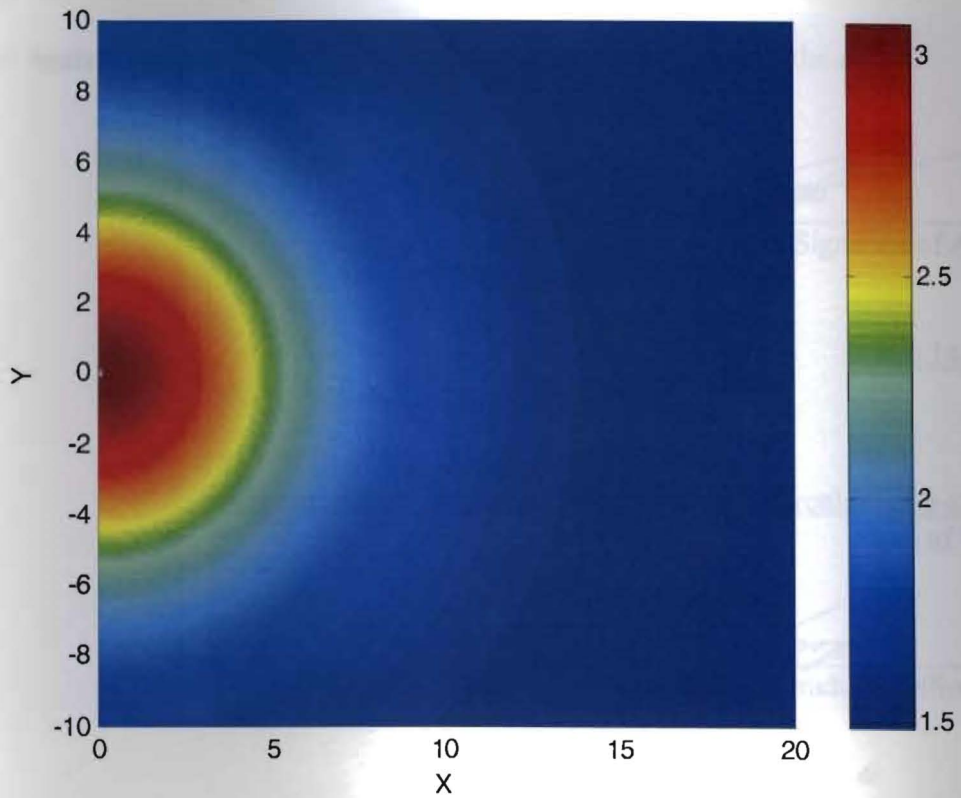
Figure 20. The percent difference between the polygonal approximation and the dipole approximation for the magnetic field "far" from a circular loop graphed as a function of x and y with $z = 10$ m.

I, Kevin Kale Grantham, hereby submit this thesis/report to Emporia State University as partial fulfillment of the requirements for an advanced degree. I agree that the Library of the University may make it available to use in accordance with its regulations governing materials of this type. I further agree that quoting, photocopying, digitizing or other reproduction of this document is allowed for private study, scholarship (including teaching) and research purposes of a nonprofit nature. No copying which involves potential financial gain will be allowed without written permission of the author.
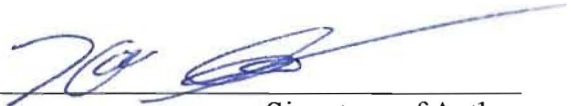
_____
Signature of Author

July 14, 2006
Date

Approximation of the Magnetic Field of a Circular Loop of Wire
Title of Thesis

_____
Signature of Graduate Office Staff

8-4-06
_____
Date Received